Comput Optim Appl (2010) 46: 535–569
DOI 10.1007/s10589-008-9201-x

A shape and topology optimization technique for solving a class of linear complementarity problems in function space

M. Hintermüller · A. Laurain

Received: 9 October 2007 / Revised: 12 August 2008 / Published online: 16 September 2008

Abstract A shape and topology optimization driven solution technique for a class of linear complementarity problems (LCPs) in function space is considered. The main motivating application is given by obstacle problems. Based on the LCP together with its corresponding interface conditions on the boundary between the coincidence or active set and the inactive set, the original problem is reformulated as a shape optimization problem. The topological sensitivity of the new objective functional is used to estimate the "topology" of the active set. Then, for local correction purposes near the interface, a level set based shape sensitivity technique is employed. A numerical algorithm is devised, and a report on numerical test runs ends the paper.

Keywords Function space · Level set method · Linear complementarity problem · Obstacle problem · Shape and topology optimization

Both authors acknowledge support by the Austrian Ministry of Science and Education and the Austrian Science Fund FWF under START-grant Y305 "Interfaces and Free Boundaries".

M. Hintermüller (✉)
University of Sussex, Falmer, Brighton, BN1 9RF, UK
e-mail: m.hintermueller@sussex.ac.uk

M. Hintermüller
Department of Mathematics, and Scientific Computing, Institute of Mathematics and Scientific Computing, University of Graz, Heinrichstr. 36, 8010 Graz, Austria

A. Laurain
Institute of Mathematics and Scientific Computing, University of Graz, Heinrichstr. 36, 8010 Graz, Austria
e-mail: antoine.laurain@uni-graz.at

1 Introduction

Linear complementarity problems (LCPs) in function space arise in many practical applications ranging from engineering science to computational finance. A prototype problem may be written as

$$Ay + \lambda = f, \quad y \leq \psi,\ \lambda \geq 0,\ \langle y - \psi, \lambda \rangle = 0, \tag{1.1}$$

where $\langle \cdot, \cdot \rangle$ denotes an appropriate pairing. Above A denotes some positive definite operator and the inequality constraint on ψ is meant in the pointwise almost everywhere sense. The realization of the non-negativity of λ depends on the regularity requirement on $y \in \mathcal{Y}$, with $\mathcal{Y}$ a Banach space. For instance, (1.1) may arise from the variational inequality (i.e., first order optimality) characterization of elliptic obstacle problems; see, e.g., [15]. In this case, A denotes a second order elliptic partial differential operator defined on the sufficiently smooth and bounded domain Ω, $f \in H^{-1}(\Omega)$ and $\psi \in H^1(\Omega)$ with $\psi_{|\partial\Omega} > 0$. The natural function space setting yields $(y, \lambda) \in (\mathcal{Y} = H_0^1(\Omega)) \times H^{-1}(\Omega)$. Under additional data regularity, however, one can show $(y, \lambda) \in (\mathcal{Y} = H^2(\Omega) \cap H_0^1(\Omega)) \times L^2(\Omega)$ such that $\lambda \geq 0$ admits a pointwise interpretation almost everywhere (a.e.) in Ω. Note that the obstacle problem is related to

$$\begin{aligned} &\text{minimize} && \frac{1}{2} a(y, y) - \langle y, f \rangle_{H_0^1, H^{-1}} \\ &\text{subject to (s.t.)} && y \leq \psi \quad \text{a.e. in } \Omega \end{aligned} \tag{1.2}$$

which admits a unique solution [15]. Here, $a : H_0^1(\Omega) \times H_0^1(\Omega) \to \mathbb{R}$ denotes the coercive and continuous bilinear form induced by A. Another example for (1.1) is related to control constrained optimal control of partial differential equations. To demonstrate this, let $B : \mathcal{Y} \to \mathcal{W}$, with a Banach space $\mathcal{W} \supset L^2(\Omega)$, denote a second order elliptic differential operator defined on the domain Ω. For a scalar $\alpha > 0$ we define $A := \alpha I + B^{-*} B^{-1}$, where B^{-*} denotes the adjoint of the solution operator B^{-1} of the underlying partial differential equation. Further define $f := B^{-*}(z - B^{-1} g)$ with data z and g as specified below. Then, for $y := u$ the LCP (1.1) is equivalent to the first order optimality system of the problem

$$\begin{aligned} &\text{minimize} && \frac{1}{2} \|w - z\|^2_{L^2(\Omega)} + \frac{\alpha}{2} \|u\|^2_{L^2(\Omega)} \\ &\text{subject to} && Bw = u + g, \qquad u \leq \psi \quad \text{a.e. in } \Omega, \end{aligned} \tag{1.3}$$

where ψ is sufficiently regular, $z \in L^2(\Omega)$ and $g \in \mathcal{W}$, and the partial differential equation has to be considered together with suitable boundary conditions. In this case, typically $\lambda \in L^2(\Omega)$ and $\lambda \geq 0$ admits a pointwise interpretation. This situation changes completely when $u \leq \psi$ in (1.3) is replaced by $w \leq \psi$, which relates to state constrained optimal control. In this case we have $y := w$ and $A := I + \alpha B^* B$ in (1.1). Then, even for very regular data, in general one only has that λ is a Borel measure such that $\lambda \geq 0$ admits no pointwise interpretation.

Concerning the development of fast solution algorithms for (1.1) we mention that low multiplier regularity (i.e., the pertinent non-negativity condition admits no pointwise interpretation) typically represents an adverse effect; see [9]. As a result numerical tools like semismooth Newton methods, which are highly efficient in the case of control constraints, admit no function space analysis and may exhibit a considerable mesh dependence. But even when $\lambda \geq 0$ admits a pointwise interpretation the necessary function space setting for (1.1) might not allow a function space version of such methods; see [8], where this is argued for the obstacle problem.

In view of the above discussion, the aim of this paper is to introduce a new perspective on versions of (1.1) lacking sufficient regularity such that fast solvers—like semismooth Newton methods—admit no function space analysis. In order to outline our idea, we note that in all of the aforementioned examples for (1.1) one may define the active and inactive sets with respect to the solution y^* of (1.1):

$$\mathcal{A}^* = \{x \in \Omega \,:\, y^*(x) = \psi(x)\}, \qquad \mathcal{I}^* = \Omega \setminus \mathcal{A}^*.$$

Then, often some closer analysis reveals additional properties of the solution on the interface $\Gamma^* = \partial\mathcal{A}^*$ between the active and inactive sets. For instance, in the case of the obstacle problem and the state constrained optimal control problem one finds

$$y^*_{|\Gamma^*} = \psi_{|\Gamma^*}, \qquad \partial_n y^*_{|\Gamma^*} = \partial_n \psi_{|\Gamma^*}, \tag{1.4}$$

where ∂_n denotes the normal derivative at Γ^*. Based on these observations, in this paper we propose an approach which considers the active and inactive sets as the unknown variables inducing corresponding y and λ, rather than vice versa as it is done in the usual approaches. This perspective allows us to dispense with the multiplier and to use tools from shape and topology optimization for solving (1.1). The algorithm which we propose follows a phase I–phase II concept, where phase I relies on topological gradients [4, 5, 25] and phase II uses tools from shape sensitivity [3, 26]. Numerically phase II further relies on a level set method [20, 21, 23] for the propagation of the geometry according to a shape sensitivity based velocity. In our tests the new algorithm exhibits a mesh independent convergence behavior. Subsequently, in the spirit of a feasibility study for an application of the new approach to state constrained optimal control, we focus on the obstacle case discussed above. In this situation (1.4) is a complete set of conditions on Γ^*.

In connection with the obstacle problem let us mention that efficient solvers based on domain or space decomposition and multigrid/multilevel methods are available; see, e.g., [14, 16–18, 27–29] and the many references therein. Let us briefly put our approach into a perspective with these methods. Space decomposition in the Jacobi variant (see, e.g., [27]) allows parallelization, but leads to restrictions in the relaxation parameter which is typically bounded by $1/m$, where m is the number of subspaces. This might yield prohibitively small update steps. The Gauss-Seidel version of this method does not suffer from this drawback, but, as for the Jacobi variant, keeping the number of subspaces fixed, leads to subproblems of obstacle type. Then, although the outer space decomposition iteration has a linear contraction rate which is independent of the number of domains and the mesh size in the discretized setting, the numerical solution of the obstacle problems becomes an issue as its solution might suffer

from mesh dependent effects. Multigrid decompositions remedy the latter effect as the subproblems are scalar only and can be solved explicitly. However, as the mesh is refined the number of subdomains grows. In [28] linear convergence is shown with a factor depending on the number ℓ of levels of nested quasi-uniform finite element partitions. The rate deteriorates as ℓ increases. On fine meshes, this might lead to a large number of multigrid cycles until successful termination. Monotone multigrid methods for obstacle problems [16–18] have an asymptotic convergence rate which grows (at most) logarithmically for decreasing mesh size. Our topology optimization based approach constitutes a technique to identify the active and inactive sets very much in the spirit of active set solvers [7, 11–13] but based on a genuine geometric concept. As a result, only elliptic partial differential equations (PDEs) need to be solved (instead of obstacle-type problems) in every iteration. For these elliptic PDEs multigrid solvers with optimal complexity are available. Our numerical experiments indicate that only a very small number of topology optimization steps is necessary to obtain a good approximation of the active set at the solution. Moreover, the iterations based on topological sensitivity appear to be rather mesh independent and, thus, preserve the optimal complexity in the case where multigrid solvers are used for the elliptic PDEs of the subproblems. However, let us emphasize that the topology optimization approach is more general as our proposed framework may also be applied, e.g., to state constrained optimal control of PDEs as outlined earlier in this section. Also, the combination of domain decomposition and topological sensitivity could be an interesting future direction.

The rest of the paper is organized as follows: In the next section we express (1.1) as a shape optimization problem and compute the corresponding topological and shape gradients, respectively. All technical details and proofs are deferred to the appendix. In Sect. 3 we introduce our new algorithm and discuss a few implementation details. Due to the combination of shape and topological sensitivity we call it TOPSHAPE algorithm. Finally, Sect. 4 provides a report on numerical tests.

2 Shape and topology optimization

For the ease of presentation, throughout we focus on the case where $A = -\Delta$, $\mathcal{Y} = H^2(\Omega) \cap H_0^1(\Omega)$ and $\psi \in H^2(\Omega)$ with $\psi_{|\partial\Omega} > 0$, i.e., the situation where (1.1) corresponds to the obstacle problem. Moreover, below we give the arguments for the two dimensional situation, but a generalization to higher dimensions is possible. In what follows we therefore assume that $\Omega \subset \mathbb{R}^2$ is a bounded domain with a Lipschitz boundary $\partial\Omega =: \Sigma$.

Subsequently we first formulate a topology optimization problem, where the wanted topology corresponds to the distribution of the active set components within the domain (in our algorithm this is phase I). In our numerics it turned out that local corrections close to the boundary of the active set are more efficient by using shape sensitivity. Consequently, we then establish a shape optimization formulation and compute shape sensitivities (phase II).

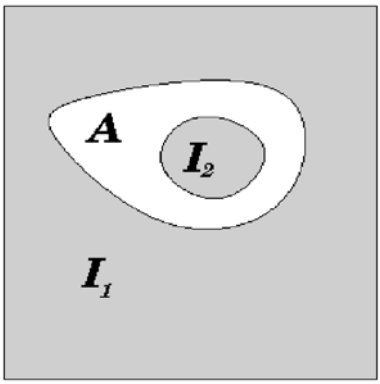

Fig. 1 Decomposition of the domain into an active region $\mathcal{A}$ and inactive regions $\mathcal{I}_1$ and $\mathcal{I}_2$

2.1 Topological optimization

We start by rewriting (1.1) as a topology optimization problem. In fact, consider the following minimization problem:

$$\begin{cases} \text{minimize} \quad J(\mathcal{I}, \mathcal{A}) \\ \text{s.t.} \quad \mathcal{I} \subset \Omega, \qquad \partial\mathcal{I} \supset \partial\Omega, \qquad \mathcal{A} = \mathcal{I}^c \subset \{f + \Delta\psi \geq 0\} \cap \Omega, \end{cases} \tag{2.5}$$

with J defined by $J(\mathcal{I}, \mathcal{A}) = \alpha_1 J_1(\mathcal{I}) + \alpha_2 J_2(\mathcal{A}) + J_3(\mathcal{I})$, with

$$J_1(\mathcal{I}) = \int_{\mathcal{I}} \max(0, \tilde{u})^2, \tag{2.6}$$

$$J_2(\mathcal{A}) = \int_{\mathcal{A}} \min(0, \tilde{v})^2, \tag{2.7}$$

$$J_3(\mathcal{I}) = \sum_{i=2}^{N} \frac{1}{|\mathcal{I}_i|} \left(\int_{\mathcal{I}_i} g \right)^2. \tag{2.8}$$

Here, α_1 and α_2 denote positive constants. The inactive set $\mathcal{I}$ is decomposed into the union of its connected components $\mathcal{I} = \bigcup_{i=1}^{N} \mathcal{I}_i$ with $\Sigma \subset \mathcal{I}_1$; see Fig. 1. The sets $\mathcal{I}_i$, $i = 2, \ldots, N$, are called *islands* and require a careful treatment as we have to solve pure Neumann problems on these islands. Indeed, the corresponding compatibility conditions lead to technical difficulties. This fact is responsible for the presence of J_3. On the other hand, we have mixed Dirichlet-Neumann conditions on $\mathcal{I}_1$, which implies existence of a unique solution of (2.10)–(2.12) below. The functions $\tilde{u}$, $\tilde{v}$ and g are defined by

$$\tilde{u} = u - \psi, \qquad \tilde{v} = v - \psi, \qquad g = f + \Delta\psi, \tag{2.9}$$

where $u = \sum_{i=1}^{N} u_i \chi_{\mathcal{I}_i}$, with χ_S the characteristic function of $S \subset \Omega$. Here u_1 solves the boundary value problem

$$-\Delta u_1(x) = f(x) \quad \text{in } \mathcal{I}_1, \tag{2.10}$$

$$u_1(x) = 0 \quad \text{on } \Sigma, \tag{2.11}$$

$$\partial_n u_1(x) = \partial_n \psi(x) \quad \text{on } \partial\mathcal{I}_1 \setminus \Sigma \tag{2.12}$$

and $\tilde{u}_i$, $i \in \{2, \dots, N\}$, solves

$$-\Delta \tilde{u}_i(x) = \bar{g}_i(x) \quad \text{in } \mathcal{I}_i, \tag{2.13}$$

$$\partial_n \tilde{u}_i(x) = 0 \quad \text{on } \partial\mathcal{I}_i, \tag{2.14}$$

with $\bar{g}_i$ defined by

$$\bar{g}_i(x) = g(x) - \frac{1}{|\mathcal{I}_i|} \int_{\mathcal{I}_i} g \quad \forall x \in \mathcal{I}_i \tag{2.15}$$

such that $\int_{\mathcal{I}_i} \bar{g}_i = 0$. Note that due to the normalization (2.15), the Neumann problem (2.13)–(2.14) admits a solution which is unique up to a constant. A solution u_i is then obtained by $u_i = \tilde{u}_i + \psi_{|\mathcal{I}_i}$ on $\mathcal{I}_i$, $i = 2, \dots, N$.

Analogously, v is the solution of

$$-\Delta v(x) = -\Delta \psi(x) \quad \text{in } \mathcal{A}, \tag{2.16}$$

$$v(x) = u(x) \quad \text{on } \partial\mathcal{A}. \tag{2.17}$$

Throughout we invoke the following assumptions:

$$\Gamma^* = \partial\mathcal{A}^* = \partial(\text{int}(\mathcal{A}^*)) = \partial\mathcal{I}^* \setminus \Sigma \subset \Omega; \tag{2.18}$$

$$\text{int}(\mathcal{A}^*) \neq \emptyset; \tag{2.19}$$

$$\mathcal{I}^* \text{ and } \text{int}(\mathcal{A}^*) \text{ allow the existence of first-order trace operators and the applicability of Greens formula [30].} \tag{2.20}$$

Next we relate (2.5) and the linear complementarity problem (1.1).

Theorem 1 (Necessary conditions) *Assume $y^* \in H^2(\Omega) \cap H_0^1(\Omega)$ is the solution of (1.1) and the active and inactive sets $\mathcal{I}^*$ and $\mathcal{A}^*$ satisfy (2.18)–(2.20). Then we have*

$$-\Delta y^* = f \quad \text{on } \mathcal{I}^*, \tag{2.21}$$

$$y^* \leq \psi \quad \text{on } \mathcal{I}^*, \tag{2.22}$$

$$y^* = 0 \quad \text{on } \Sigma, \tag{2.23}$$

$$y^* = \psi \quad \text{on } \Gamma^*, \tag{2.24}$$

$$\partial_n y^* = \partial_n \psi \quad \text{on } \Gamma^*, \tag{2.25}$$

$$f + \Delta\psi \geq 0 \quad \text{on } \mathcal{A}^*, \tag{2.26}$$

$$J(\mathcal{I}^*, \mathcal{A}^*) = 0. \tag{2.27}$$

(Sufficient conditions) *Assume conversely that we have found an open set $\hat{\mathcal{I}}$ with $\Sigma \subset \hat{\mathcal{I}}$. We set $\hat{\Gamma} = \partial\hat{\mathcal{I}} \setminus \Sigma$ and assume that $\hat{\mathcal{I}}$ and $\hat{\mathcal{A}} = \hat{\mathcal{I}}^c \subset \{f + \Delta\psi \geq 0\} \cap \Omega$*

satisfy (2.18)–(2.20). *Let* $\hat{u}$ *and* $\hat{v}$ *denote the associated solutions corresponding to* (2.10)–(2.12), (2.16)–(2.17) *and* (2.13)–(2.14). *If* $J(\hat{\mathcal{I}}, \hat{\mathcal{A}}) = 0$, *then* $\hat{y}$ *defined by*

$$\hat{y} = \begin{cases} \hat{u} & \text{on } \hat{\mathcal{I}}, \\ \hat{v} & \text{on } \hat{\mathcal{A}} \end{cases} \tag{2.28}$$

is the unique solution of (1.1), *i.e.*, $\hat{y} = y^*$.

Proof (Necessary conditions) If y^* is the solution the obstacle problem (1.2) we first observe $\bar{g}_i = g_{|\mathcal{I}_i}$ on $\mathcal{I}_i^*$, $i = 2, \ldots, N$, since the solution y^* solves a pure Neumann problem with right-hand side f on $\mathcal{I}_i^*$, $i = 2, \ldots, N$. Next let $u^* = y^*$ on $\mathcal{I}^*$, hence $u^* = \psi$ on $\partial\mathcal{I}_i^*$, and $v^* = y^*$ on $\mathcal{A}^*$, then (2.10)–(2.12), (2.13)–(2.14) and (2.16)–(2.17) are satisfied. Further

$$\begin{aligned} u^* \le \psi \quad \text{in } \mathcal{I}^* &\Longrightarrow J_1(\mathcal{I}^*) = 0, \\ v^* = \psi \quad \text{in } \mathcal{A}^* &\Longrightarrow J_2(\mathcal{A}^*) = 0, \\ \int_{\mathcal{I}_i^*} g = 0,\ i = 2, \ldots, N &\Longrightarrow J_3(\mathcal{I}^*) = 0. \end{aligned}$$

(Sufficient conditions) Since $J(\hat{\mathcal{I}}, \hat{\mathcal{A}}) = 0$, we get

$$\hat{u} \le \psi \quad \text{in } \hat{\mathcal{I}}, \tag{2.29}$$

$$\hat{v} \ge \psi \quad \text{in } \hat{\mathcal{A}}, \tag{2.30}$$

$$\int_{\hat{\mathcal{I}}_i} g = 0 \quad \text{in } \hat{\mathcal{I}}_i,\ i = 2, \ldots, N. \tag{2.31}$$

According to (2.29) and (2.17) and since $\hat{\mathcal{I}}$ and $\hat{\mathcal{A}}$ are assumed to be sufficiently smooth, $\hat{v} \le \psi$ on $\partial\hat{\mathcal{A}}$, which leads to $\hat{v} \le \psi$ in $\hat{\mathcal{A}}$ and, together with (2.30), $\hat{v} = \psi$ in $\hat{\mathcal{A}}$. In view of (2.31), $\bar{g}_i = g_{|\mathcal{I}_i}$ on $\hat{\mathcal{I}}_i$, $i = 2, \ldots, N$. Then $\hat{y}$ satisfies the conditions (2.21)–(2.25). Equation (2.26) is fulfilled due to $\hat{\mathcal{A}} \subset \{f + \Delta\psi \ge 0\}$. Therefore $\hat{y}$ is the solution of the obstacle problem (1.2) and, hence, solves (1.1). □

Note that condition (2.31) is crucial in the case of islands. If it would not hold, then we would have a feasible solution, but for a modified source term $\bar{g}$. This would imply that a different obstacle problem were solved.

2.1.1 Topological derivative

For given inactive and active sets $\mathcal{I}$ and $\mathcal{A}$, the topological derivative measures the variation of J when a small subdomain of $\mathcal{I}$ becomes active or when a small subdomain of $\mathcal{A}$ becomes inactive. For instance, for demonstrating the first case above assume that $\mathcal{I} = \Omega$ and $\mathcal{A} = \emptyset$. Let ω be the ball of (sufficiently small) radius ε and

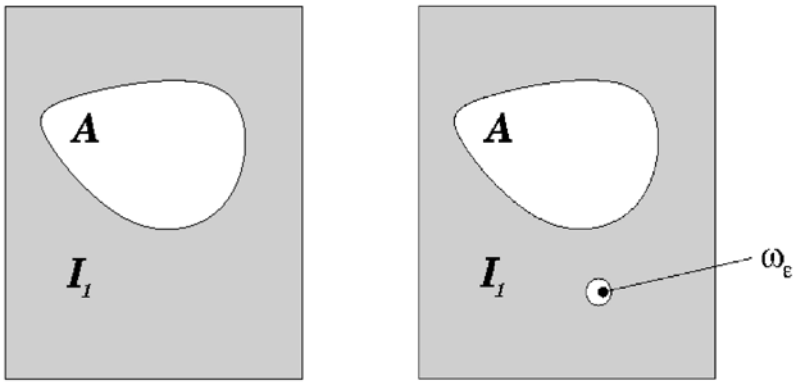

Fig. 2 Introduction of a new active components ω_ε to the active set $\mathcal{A}$

of center $x_0 \in \mathcal{I}$. We define the perturbed domains $\mathcal{I}_\varepsilon$, $\mathcal{A}_\varepsilon$ and ω_ε in the following way: $\omega_\varepsilon := \{x \in \mathbb{R}^2 : \ x = \varepsilon\xi, \ \xi \in \omega\}$, $\mathcal{I}_\varepsilon := \mathcal{I} \setminus \omega_\varepsilon$ and $\mathcal{A}_\varepsilon := \omega_\varepsilon$. Then, as $\varepsilon \downarrow 0$ we have the expansion:

$$J(\mathcal{I}_\varepsilon, \mathcal{A}_\varepsilon) = J(\mathcal{I}, \mathcal{A}) + \pi\varepsilon^2 \mathcal{T}(x_0) + o(\varepsilon^2), \tag{2.32}$$

where $\mathcal{T}(x_0)$ is the so-called *topological derivative of J at x_0*; see Fig. 2 for a graphical illustration. In fact, we define such topological derivatives $\mathcal{T}_1$,$\mathcal{T}_2$ and $\mathcal{T}_3$ for each functional J_1, J_2 and J_3, respectively. The topological derivative $\mathcal{T}$ of J is then given by

$$\mathcal{T} = \alpha_1 \mathcal{T}_1 + \alpha_2 \mathcal{T}_2 + \mathcal{T}_3. \tag{2.33}$$

Due to our decomposition of Ω into active and inactive sets, the following three situations may occur when changing a small subset from one set to the other. In what follows, due to the structure of ω we refer to these small subsets as holes in the respective set.

Case 1 "Active hole in inactive set". A small active region is created in the inactive region $\mathcal{I}_1$. Due to our initialization, in the first iteration of our algorithm we are only concerned with this case.

Case 2 "Inactive hole in active set". A small inactive region is created in the active set $\mathcal{A}$.

Case 3 "Active hole in inactive island". A small active region is created in the inactive island $\mathcal{I}_i$, $i = 2, \ldots, N$.

The topological derivatives $\mathcal{T}_1$, $\mathcal{T}_2$ and $\mathcal{T}_3$ for the cases introduced above are gathered in Table 1, where $\bar{p}_u(x)$ is defined analogously to (2.15). The topological derivative $\mathcal{T}$ can then be recovered by using (2.33). Note that in a slight misuse of notation

Table 1 The topological derivative in case 1–3

	$\mathcal{T}_1(x)$
Case 1	$2\nabla\tilde{u}(x)\cdot\nabla p_u(x) - p_u(x)g(x) - \max(0,\tilde{u}(x))^2$
Case 2	$\max(0,\tilde{v}(x))^2$
Case 3	$2\nabla\tilde{u}(x)\cdot\nabla p_u(x) - \bar{p}_u(x)\bar{g}(x) - \max(0,\tilde{u}(x))^2$
	$\mathcal{T}_2(x)$
Case 1	$\min(0,\tilde{v}(x))^2$
Case 2	$2\nabla\tilde{v}(x)\cdot\nabla p_v(x) - \min(0,\tilde{v}(x))^2$
Case 3	$\min(0,\tilde{v}(x))^2$
	$\mathcal{T}_3(x)$
Case 1	0
Case 2	$g(x)^2$
Case 3	$\frac{1}{\lvert\mathcal{I}_i\rvert}\left(\int_{\mathcal{I}_i} g\right)\cdot\left(\frac{1}{\lvert\mathcal{I}_i\rvert}\int_{\mathcal{I}_i} g - 2g(x)\right)$

we leave out the indices i in the island case. The detailed derivation is provided in Appendix A. The adjoint states p_u and p_v solve the following problems:

$$-\Delta p_v(x) = 2\min(0, v(x) - \psi(x)) \quad \text{in } \mathcal{A}, \tag{2.34}$$

$$p_v(x) = 0 \quad \text{on } \partial\mathcal{A}, \tag{2.35}$$

as well as

$$-\Delta p_u(x) = 2\max(0, u(x) - \psi(x)) \quad \text{in } \mathcal{I}_1, \tag{2.36}$$

$$p_u(x) = 0 \quad \text{on } \Sigma, \tag{2.37}$$

$$\partial_{n_\mathcal{I}} p_u(x) = -\partial_{n_\mathcal{A}} p_v(x) \quad \text{on } \partial\mathcal{I}_1 \setminus \Sigma, \tag{2.38}$$

and further (with some slight misuse of notation)

$$-\Delta p_u(x) = 2\max(0, u(x) - \psi(x)) \quad \text{in } \mathcal{I}_i,\ i = 2,\dots,N, \tag{2.39}$$

$$\partial_{n_\mathcal{I}} p_u(x) = -\partial_{n_\mathcal{A}} p_v(x) \quad \text{on } \partial\mathcal{I}_i,\ i = 2,\dots,N, \tag{2.40}$$

where $n_\mathcal{I}$ and $n_\mathcal{A}$ are the outward unit normal vectors to $\mathcal{I}$ and $\mathcal{A}$, respectively. Since (2.39)–(2.40) is a pure Neumann problem it must satisfy the compatibility condition

$$\int_{\mathcal{I}_i} \max(0,\tilde{u}) = -\int_{\mathcal{A}} \min(0,\tilde{v}), \quad i = 2,\dots,N, \tag{2.41}$$

which contributes to the normalization of the system (2.13)–(2.14).

2.2 Shape optimization

For shape sensitivity we assume that the boundary of $\mathcal{I}$ is split into its connected components $\partial\mathcal{I} = \Sigma \cup \Gamma$, $\Gamma = \bigcup_{i=1}^{N} \Gamma_i$. Then we consider the following problem:

$$\begin{cases} \text{minimize} \quad K(\mathcal{I}, \mathcal{A}) \\ \text{s.t.} \quad \mathcal{I} \subset \Omega, \qquad \partial\mathcal{I} \supset \partial\Omega, \qquad \mathcal{A} = \mathcal{I}^c \subset \Omega, \end{cases} \tag{2.42}$$

with $K(\mathcal{I}, \mathcal{A}) = \alpha_1 K_1(\mathcal{I}) + \alpha_2 K_2(\mathcal{A}) + K_3(\mathcal{I})$, and

$$K_1(\mathcal{I}) = \int_{\mathcal{I}} \max(0, \tilde{u})^2, \tag{2.43}$$

$$K_2(\mathcal{A}) = \sum_{i=1}^{N} \frac{1}{|\Gamma_i|} \int_{\Gamma_i} |\partial_n \tilde{u}|^2, \tag{2.44}$$

$$K_3(\mathcal{I}) = \int_{\mathcal{A}} \min(0, g)^2. \tag{2.45}$$

The functions $\tilde{u}$ and g are defined as in (2.9), but now with $u = \tilde{u} + \psi$ solving

$$-\Delta u(x) = f(x) \quad \text{in } \mathcal{I}, \tag{2.46}$$

$$u(x) = 0 \quad \text{on } \Sigma, \tag{2.47}$$

$$u(x) = \psi(x) \quad \text{on } \partial\mathcal{I} \setminus \Sigma. \tag{2.48}$$

Note that we do not have a problem defined on $\mathcal{A}$ since the solution is now forced to be ψ on this set. The functional K_3 is a relaxation of the requirement $\lambda = f + \Delta\psi \geq 0$ on the active set $\mathcal{A}$. Alternatively, this condition may be satisfied by including $\mathcal{A} \subset \{f + \Delta\psi\} \cap \Omega$ in the formulation of (2.42).

Theorem 2 (Necessary conditions) *Assume $y^* \in H^2(\Omega) \cap H_0^1(\Omega)$ is the solution of (1.1), and the active and inactive sets $\mathcal{I}^*$ and $\mathcal{A}^*$ satisfy (2.18)–(2.20). Then (2.21)–(2.27) and $K(\mathcal{I}^*, \mathcal{A}^*) = 0$ are satisfied.*

(Sufficient conditions) *Assume conversely that we have found an open set $\hat{\mathcal{I}}$ with $\Sigma \subset \hat{\mathcal{I}}$. We set $\hat{\Gamma} = \partial\hat{\mathcal{I}} \setminus \Sigma$ and assume that $\hat{\mathcal{I}}$ and $\hat{\mathcal{A}} = \hat{\mathcal{I}}^c$ satisfy (2.18)–(2.20). Let $\hat{u}$ denote the associated solution corresponding to (2.46)–(2.48). If $K(\hat{\mathcal{I}}, \hat{\mathcal{A}}) = 0$, then $\hat{y}$ defined by*

$$\hat{y} = \begin{cases} \hat{u} & \text{on } \hat{\mathcal{I}}, \\ \psi & \text{on } \hat{\mathcal{A}} \end{cases} \tag{2.49}$$

is the unique solution of (1.1), i.e., $\hat{y} = y^*$.

Proof Let y^* denote the solution of (1.1). Then $u^* := y^*$ is the solution of (2.46)–(2.48) on $\mathcal{I}^*$. Further we find $K(\mathcal{I}^*, \mathcal{A}^*) = 0$. On the other hand, if $(\hat{\mathcal{I}}, \hat{\mathcal{A}})$ is a solu-

tion of (2.42) with $K(\hat{\mathcal{I}}, \hat{\mathcal{A}}) = 0$, then we get for the corresponding $\hat{u}$

$$\hat{u} \le \psi \quad \text{in } \hat{\mathcal{I}}, \tag{2.50}$$

$$\partial_n \hat{u} = \partial_n \psi \quad \text{on } \hat{\Gamma}_i,\ i = 2, \dots, N, \tag{2.51}$$

$$g \ge 0 \quad \text{in } \hat{\mathcal{A}}. \tag{2.52}$$

Thus, $\hat{y}$ is a solution of the obstacle problem (1.1). The condition $\lambda = f + \Delta\psi \ge 0$ on the active set $\hat{\mathcal{A}}$ is guaranteed by (2.52). □

2.2.1 *Shape gradient*

Below, the quantities $\mathcal{S}_1$, $\mathcal{S}_2$, $\mathcal{S}_3$ stand for the shape gradients of K_1, K_2 and K_3, respectively. Let V be a vector field in $\mathcal{C}([0, T]; \mathcal{C}^2(\Omega, \mathbb{R}^2))$. According to the results of [26], the shape derivative $\tilde{u}'$ of $\tilde{u}$ is the solution of

$$-\Delta\tilde{u}'(x) = 0 \quad \text{in } \mathcal{I}, \tag{2.53}$$

$$\tilde{u}'(x) = 0 \quad \text{on } \Sigma, \tag{2.54}$$

$$\tilde{u}'(x) = -\partial_n \tilde{u}\, v_n \quad \text{on } \partial\mathcal{I} \setminus \Sigma, \tag{2.55}$$

with $v_n = V(0) \cdot n$ and n the outward unit normal vector to $\mathcal{I}$. The shape gradient of K_1 is given by

$$\mathcal{S}_1(\mathcal{I}, \mathcal{A}; V) = \int_{\mathcal{I}} 2\max(0, \tilde{u})\tilde{u}' + \int_{\Gamma} \max(0, \tilde{u})^2 v_n.$$

Introducing the adjoint state

$$-\Delta p_1 = 2\max(0, \tilde{u}) \quad \text{in } \mathcal{I}, \tag{2.56}$$

$$p_1 = 0 \quad \text{on } \partial\mathcal{I}, \tag{2.57}$$

we obtain from Green's formula

$$\mathcal{S}_1(\mathcal{I}, \mathcal{A}; V) = \int_{\Gamma} [\partial_n p_1 \partial_n \tilde{u} + \max(0, \tilde{u})^2] v_n. \tag{2.58}$$

For our calculation, K_2 is written as the product

$$K_2(\Gamma) = \sum_{i=1}^{N} L_1(\Gamma_i) L_2(\Gamma_i)$$

with

$$L_1(\Gamma_i) = \frac{1}{|\Gamma_i|}, \qquad L_2(\Gamma_i) = \int_{\Gamma_i} |\partial_n \tilde{u}|^2.$$

The shape gradient of L_1 is then given by

$$\mathcal{S}_{L_1}(\Gamma_i; V) = -\frac{1}{|\Gamma_i|^2} \int_{\Gamma_i} \mathcal{H}_i v_n,$$

where $\mathcal{H}_i$ stands for the curvature of Γ_i. Further, the shape gradient of L_2 is given by

$$\mathcal{S}_{L_2}(\Gamma_i; V) = \int_{\Gamma_i} \left(2\partial_n \tilde{u} \partial_n \tilde{u}' - g\tilde{u} v_n + \mathcal{H}_i |\partial_n \tilde{u}|^2 v_n\right),$$

so that

$$\begin{aligned}&\mathcal{S}_2(\mathcal{I}, \mathcal{A}; V)\\ &= \sum_{i=1}^{N} \int_{\Gamma_i} \left(2L_1(\Gamma_i)\partial_n \tilde{u} \partial_n \tilde{u}' - \left[L_1(\Gamma_i)(g\tilde{u} - \mathcal{H}_i |\partial_n \tilde{u}|^2) + \frac{L_2(\Gamma_i)}{|\Gamma_i|^2}\mathcal{H}_i\right] v_n\right).\end{aligned}$$

Introducing the adjoint state

$$-\Delta p_2 = 0 \quad \text{in } \mathcal{I}, \tag{2.59}$$

$$p_2 = 2L_1(\Gamma_i)\partial_n \tilde{u} \quad \text{on } \Gamma_i, \tag{2.60}$$

$$p_2 = 0 \quad \text{on } \Sigma, \tag{2.61}$$

we get from Green's formula

$$\int_{\mathcal{I}} -\Delta p_2 \tilde{u}' = \int_{\mathcal{I}} -\Delta \tilde{u}' p_2 - \int_{\partial \mathcal{I}} \left(\partial_n p_2 \tilde{u}' - p_2 \partial_n \tilde{u}'\right).$$

In view of (2.59)–(2.61), (2.53)–(2.55) this leads to

$$-\sum_{i=1}^{N} \int_{\Gamma_i} \partial_n p_2 \partial_n \tilde{u} v_n = \sum_{i=1}^{N} \int_{\Gamma_i} 2L_1(\Gamma_i)\partial_n \tilde{u} \partial_n \tilde{u}'.$$

Finally we obtain

$$\mathcal{S}_2(\mathcal{I}, \mathcal{A}; V) = \sum_{i=1}^{N} \int_{\Gamma_i} -\left[\partial_n p_2 \partial_n \tilde{u} + L_1(\Gamma_i)(g\tilde{u} - \mathcal{H}_i |\partial_n \tilde{u}|^2) + \frac{L_2(\Gamma_i)}{|\Gamma_i|^2}\mathcal{H}_i\right] v_n. \tag{2.62}$$

The calculation of the shape gradient of K_3 is straightforward since g does not depend on the shape of the domain:

$$\mathcal{S}_3(\mathcal{I}, \mathcal{A}; V) = -\int_{\Gamma} \min(0, g)^2 v_n. \tag{2.63}$$

The minus sign in (2.63) is due to the direction of the normal vector n (the integral is defined over the active set $\mathcal{A}$ in K_3).

The overall shape derivative of K is given by $\mathcal{S} = \alpha_1 \mathcal{S}_1 + \alpha_2 \mathcal{S}_2 + \mathcal{S}_3$. As all $\mathcal{S}$ are linear in V, which is arbitrary, subsequently we skip V in the notation of the shape derivative.

3 TOPSHAPE algorithm

In this section we introduce the discretized version of the algorithm for the $2d$-problem and discuss details of its implementation. The algorithm is composed of two separate parts: First we use topology optimization to find an approximate active set. This phase is usually fast but it suffers from local effects near the optimal active and inactive set. The fine adjustment is done by shape sensitivity in a second step using a level set method [21]. In what follows the level set function will be denoted by ϕ. Its zero-level set represents $\partial\mathcal{A}$. Further we suppose that $\phi < 0$ in $\mathcal{A}$ and $\phi > 0$ in $\mathcal{I}$. It is well-known (see, e.g., [21]) that the zero-level may be advanced in normal direction with a velocity F by performing time steps in the level set equation

$$\phi_t + F\|\nabla\phi\| = 0 + \text{initial conditions}.$$

In our context, the level set function is chosen to be the signed distance function.

3.1 The discrete algorithm

In the subsequent algorithm for all quantities superscript h refers to the discrete counterpart of the respective continuous variable.

Phase I: TOPology optimization algorithm

Step 1. Set $\mathcal{A}_0^h := \emptyset$ and $n := 0$; select a stopping tolerance $\gamma_t > 0$.

Step 2. Compute (u_n^h, v_n^h) as solution to (2.10)–(2.12), (2.13)–(2.14) and (2.16)–(2.17).

Step 3. Evaluate the cost functional $J^h(\mathcal{I}_n^h, \mathcal{A}_n^h)$ and compute its topological derivative $\mathcal{T}^h(x)$ at every point $x \in \Omega^h$. If $\|\mathcal{T}^h\| < \gamma_t$ then stop; otherwise continue with step 4.

Step 4. Update $\mathcal{I}_n^h$ and $\mathcal{A}_n^h$ depending on the value of the topological derivative $\mathcal{T}^h(x)$. Put $n := n + 1$ and go to step 2.

Phase II: SHAPE optimization algorithm

Step 1. Start with $\mathcal{I}_0^h$, $\mathcal{A}_0^h$ and Γ_0^h given by the topology optimization algorithm; set $n := 0$ and select a stopping tolerance $\gamma_t > \gamma_s > 0$.

Step 2. Compute u_n^h by solving (2.46)–(2.48).

Step 3. Evaluate the cost functional $K^h(\mathcal{I}_n^h, \mathcal{A}_n^h)$ and compute its shape derivative $\mathcal{S}^h(\mathcal{I}_n^h, \mathcal{A}_n^h)$. If $\|\mathcal{S}^h(\mathcal{I}_n^h, \mathcal{A}_n^h)\| < \gamma_s$ then stop; otherwise continue with step 4.

Step 4. Use an appropriate extension of $-\mathcal{S}^h(\mathcal{I}_n^h, \mathcal{A}_n^h)$ to Ω^h as a speed function in the discrete level set equation for updating the level set function ϕ_n^h.

Step 5. Set Γ_{n+1}^h equal to the zero level set of the updated level set function ϕ_{n+1}^h, and put $n := n + 1$. Go to step 2.

3.2 Aspects of the implementation

The discretization of the state system as well as the adjoint equations can be based on either finite differences or finite elements, and it is to some extent independent of the

discretization of the level set equation. Below we concentrate on a finite difference discretizations for both. We assume that the discretized domain is given by a uniform grid with mesh size h. The grid points are denoted by $\mathbf{x}_i$, $i = 1, \ldots, N$. For the discretization of the Laplace operator we use the standard five point stencil with an appropriate modification near the interface Γ_h where Neumann conditions occur. The grid functions $u^h, v^h, \psi^h, \ldots$ are defined on the grid points. The level set equation is discretized on the same grid. By ϕ^h we denote the discrete level set function defined on the grid points.

3.2.1 Topology optimization algorithm

Step 2. The solution (u_n^h, v_n^h) of the discrete system corresponding to (2.10)–(2.12) and (2.16)–(2.17) has to be computed. Due to the Neumann conditions for the system (2.10)–(2.12), we modify the stencil by using a *mirror imaging* technique [24] near the boundary, which consists of points in the discrete active set $\mathcal{A}_n^h$. The numerical solution of the Neumann problems on islands follows standard procedures; see, e.g., [6]. On each island, the normalization of the solution is done by subtracting the maximal value of the discrete solution $\tilde{u}^h$ corresponding to (2.13)–(2.14) with mean value zero. As a consequence, on every island the solution is below the obstacle.

Step 3. For computing the value of the discretized topological derivative $\mathcal{T}^h(x)$ we have to solve the adjoint equations (2.34)–(2.35), (2.36)–(2.38) and (2.39)–(2.40). The treatment is as described in step 2. We assume that the topological derivative can be extended to the boundaries. Such an assumption has a theoretical background; see for instance [2]. It is not necessary to compute the topological derivative on the boundary if we perform only one step in phase I. But when proceeding to several steps, we have to invoke such an extension. From a numerical point of view, this is delicate because we have to compute gradients on the boundary. In order to circumvent this, we instead define interior neighbors to boundary points and set the gradient on the boundary equal to the gradient at these neighbor points.

Step 4. Assuming that $\min_{y\in\Omega} \mathcal{T}(y) < 0$, we modify a point x only if $\mathcal{T}(x) \leq (1-\alpha)\min_{y\in\Omega}\mathcal{T}(y)$ with $\alpha \in (0,1)$. A modification of a point refers to switching from active to inactive or vice versa. Note that for $\alpha = 1$ we modify the nature of the point whenever $\mathcal{T}$ is negative. This choice turns out to be too aggressive in most cases. The best results are attained when the value of α is adapted during the iterations. In fact, employing a line search procedure allows to choose a value of α at every iteration such that the objective function sufficiently decreases. In this procedure, one starts with an arbitrary $\alpha_0 > 0$ (numerically, the initial value $\alpha_0 = 0.5$ seems to give good results). Then, given $\nu > 0$, $0 < \beta < 1$ and $\alpha_{\ell-1}$ for $\ell \geq 1$, the line search procedure in iteration n reduces α by $\alpha_\ell = \beta\alpha_{\ell-1}$ as long as

$$J^h(\mathcal{I}^h(\alpha_\ell), \mathcal{A}^h(\alpha_\ell)) - J^h(\mathcal{I}_{n-1}^h, \mathcal{A}_{n-1}^h) \leq -\nu\alpha\|\mathcal{T}_n^h\|_{L_2(\Omega)}^2 \tag{3.64}$$

is not satisfied. Here $\mathcal{I}^h(\alpha_\ell), \mathcal{A}^h(\alpha_\ell)$ denote the sets induced by α_ℓ. As soon as (3.64) is satisfied we set $\mathcal{I}_n^h := \mathcal{I}^h(\alpha_\ell)$ and analogously for $\mathcal{A}_n^h$. In the examples below, we use $\beta = 0.6$ and $\nu = 10^{-2}$.

3.2.2 *Shape optimization algorithm*

Step 1 and *Step 2* are similar to the ones of phase I. The major difference is that now Dirichlet (instead of Neumann) boundary conditions have to considered.

Step 3. Due to the Dirichlet boundary conditions, the product of the normal derivatives in the shape gradient formulas (2.58) and (2.62) can be written as the scalar product of the gradient. Therefore, we only need to compute the gradient as in step 3 of the topology optimization algorithm. The curvature which is also involved in the shape gradient is computed as the Laplacian of the level set function. This is possible since ϕ is chosen to be the signed distance function; see [23] for technical details.

Step 4. The level set equation is discretized in space by a first order upwind scheme and in time by a first order explicit Euler method [20, 21]. The time discretization is combined with a line search procedure, which allows us to relax the step size restriction due to the CFL-condition; see [10] for further details. Since the shape gradient is defined on Γ, but the level set equation is considered in Ω, an extension velocity V_{ext} has to be computed. We use

$$\nabla V_{\text{ext}} \cdot \nabla \phi = 0 \quad \text{in } \mathbb{R}^+ \times \Omega; \tag{3.65}$$

see [31]. By this choice, ϕ will (approximately) satisfy $|\nabla \phi| = 1$. The numerical realization of (3.65) is done by employing a time stepping scheme for an associated Hamilton-Jacobi-type equation until steady state; see [20, 22]. A similar technique is used for re-initialization of ϕ. In fact, due to numerical errors ϕ might lose its signed-distance character, and the re-initialization will modify ϕ to be a signed distance function again.

4 Numerical results

Next we report on numerical results obtained by the TOPSHAPE-algorithm. Unless mentioned otherwise we have $\Omega = (0, 1)^2$. In the tables below, the second column shows the number of iterations consumed by the topology optimization part (phase I), and the last column depicts the correspond iteration number of phase II, the shape optimization part, of the TOPSHAPE algorithm.

Example 1 This example features a non-symmetric and convex active set and no inactive islands. The problem data are $f(x_1, x_2) = 70$, $\psi(x_1, x_2) = x_2 x_1^2 + 1.2$, $\alpha_1 = 0.8$, $\alpha_2 = 0.5$. The numerical solution and the pertinent active set are shown in Fig. 3, and Table 2 depicts the iteration numbers.

Example 2 The data are $f(x_1, x_2) = 70$, $\psi(x_1, x_2) = 0.3\cos(4\pi(x_1 - 0.5)) \times \cos(4\pi(x_2 - 0.5)) + 1.2$, $\alpha_1 = 0.6$, $\alpha_2 = 0.5$. From Fig. 4 we observe that the inactive set at the numerical solution as two connected components. Hence, this reflects an "island" case, where on the inactive island a Neumann problem has to be solved. Table 3 shows the corresponding iteration numbers.

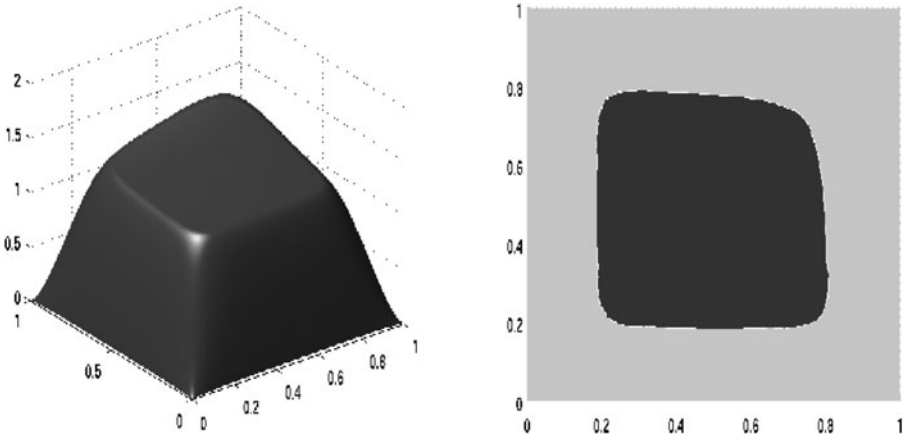

Fig. 3 Example 1. Solution u_h (*left*) and its corresponding active set (*right*)

Table 2 Example 1. Display of iteration numbers of TOPSHAPE

h	#it(topolog.)	#it(shape)
1/128	6	1
1/256	3	1
1/512	3	2

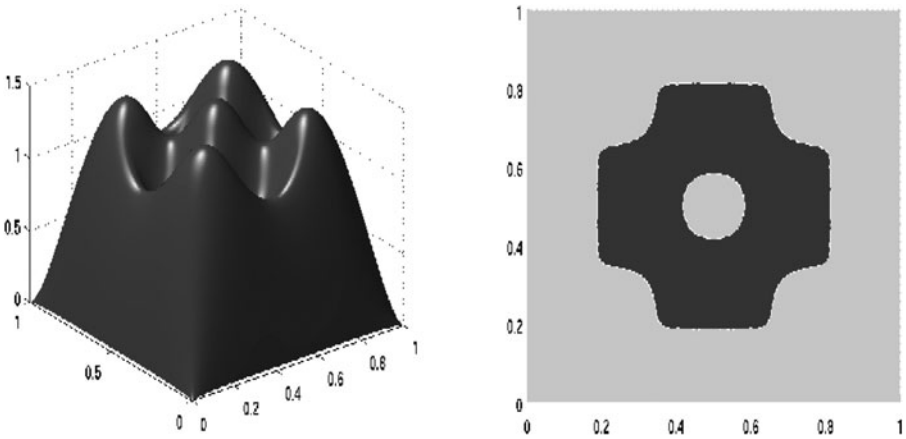

Fig. 4 Example 2. Solution u_h (*left*) and its corresponding active set (*right*)

Example 3 In this case we have $f(r,\theta) = 30(2\cos(8\pi r) + 1)\mathbf{1}_{\{r<0.4\}}$ in polar coordinates, $\psi(x_1, x_2) = 0.7$, $\alpha_1 = 0.6$, $\alpha_2 = 0.5$. Figure 5 indicates that the active as well as inactive sets consist of two connected components. Hence, as in Example 2 an "island" case occurs. The iteration numbers are shown in Table 4. For this example there is a balance of topology and shape iterations at a very low level.

Table 3 Example 2. Display of iteration numbers of TOPSHAPE

h	#it(topolog.)	#it(shape)
1/128	2	1
1/256	2	4
1/512	4	6

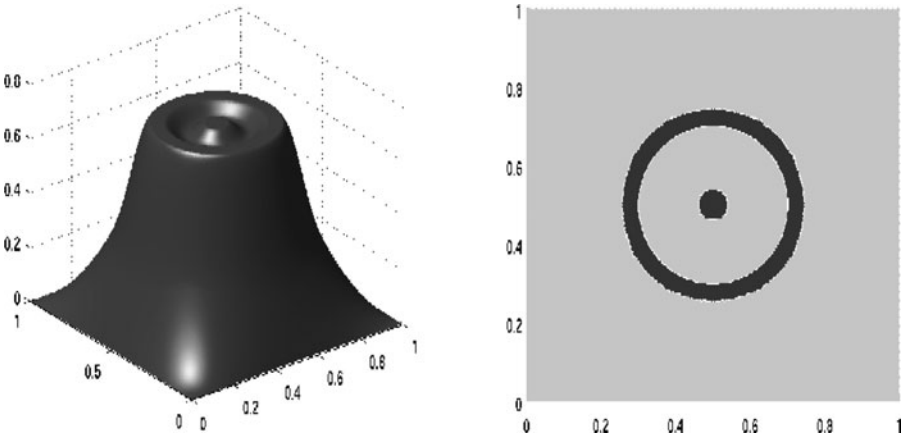

Fig. 5 Example 3. Solution u_h (*left*) and its corresponding active set (*right*)

Table 4 Example 3. Display of iteration numbers of TOPSHAPE

h	#it(topolog.)	#it(shape)
1/128	2	2
1/256	4	2
1/512	3	4

Example 4 The next example is a non-symmetric island case as can be seen from Fig. 6. The data for this example is $f(r,\theta) = 30(2\cos(8\pi r) + 1)\mathbf{1}_{\{0.1<r<0.4\}}$ again in polar coordinates, $\psi(x_1, x_2) = 0.4 + 0.5x_1$, $\alpha_1 = 0.6$, $\alpha_2 = 0.5$. The number of iterations can be found in Table 5.

Example 5 The last example is constructed explicitly and, thus, allows us to study the accuracy of the algorithm. Now, Ω is given by a disc with radius $a_3 > 0$. We further assume that ψ is a constant obstacle. The source term f is chosen to be

$$f(r,\theta) = \beta\left(r - \frac{2a_1}{3}\right) \quad \text{in } B\left(0, \frac{a_1 + a_2}{2}\right), \tag{4.66}$$

$$f(r,\theta) = \psi\left(\frac{a_2^2}{2}\ln\left(\frac{a_2}{a_3}\right) + \frac{a_3^2 - a_2^2}{4}\right)^{-1} \quad \text{in } B\left(\frac{a_1 + a_2}{2}, a_3\right), \tag{4.67}$$

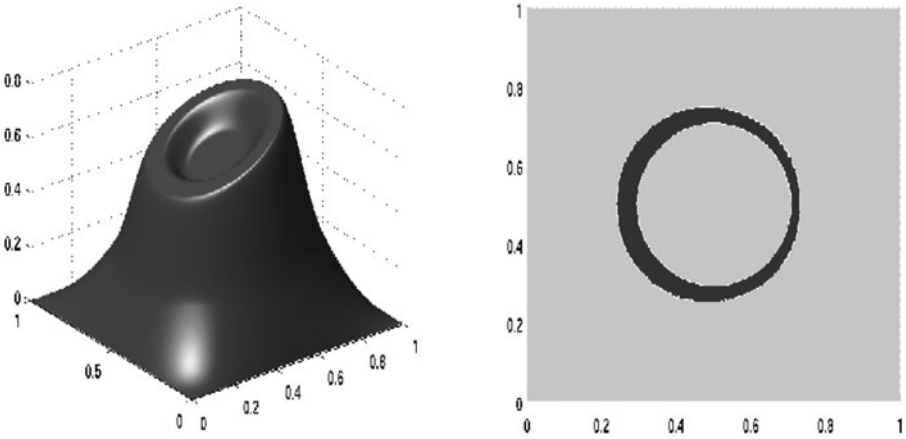

Fig. 6 Example 4. Solution u_h (*left*) and its corresponding active set (*right*)

Table 5 Example 4. Display of iteration numbers of TOPSHAPE

h	#it(topolog.)	#it(shape)
1/128	3	1
1/256	4	3
1/512	8	5

where $r = (x_1 + x_2)^{1/2}$ and $0 < a_1 < a_2 < a_3$. Then the solution of the obstacle problem (1.1) is given by

$$u(r,\theta) = \psi - \frac{\beta}{18}(2r + a_1)(r - a_1)^2 \quad \text{in } B(0,a_1), \tag{4.68}$$

$$u(r,\theta) = \psi \quad \text{in } B(a_1,a_2), \tag{4.69}$$

$$u(r,\theta) = \frac{f(r,\theta)}{4}\left(2a_2^2 \ln\left(\frac{r}{a_3}\right) + a_3^2 - r^2\right) \quad \text{in } B(a_2,a_3). \tag{4.70}$$

Thus, the active set is $B(a_1,a_2)$, and we can verify that $u < \psi$ on the inactive set $B(0,a_1) \cup B(a_2,a_3)$.

For our numerical realization we choose $a_1 = 1/4$, $a_2 = 1/2$, $a_3 = 1$, and $\psi \equiv 1$. In the subsequent table, the explicit solution is called u_{ex} and the solution obtained by the TOPSHAPE-algorithm is called u_{ts}. The corresponding active and inactive sets are denoted similarly.

In Table 6, for each mesh size h we print the objective value of J and the distance in $H^1(B(0,a_3))$ of u_{ts} to the explicit solution u_{ex}, respectively. We also present the number of iterations required. Note that the approximation error is of the order of the mesh size of our discretization.

Table 6 Example 5. Objective values (upon termination), H_1-distances and iteration numbers of TOPSHAPE

	$h = 1/128$	$h = 1/256$	$h = 1/512$
$J(I_{ex}, \mathcal{A}_{ex})$	6.67×10^{-6}	1.54×10^{-6}	3.63×10^{-7}
$J(I_{ts}, \mathcal{A}_{ts})$	8.78×10^{-6}	3.70×10^{-6}	7.65×10^{-7}
$\|u_{ts} - u_{ex}\|_{H^1}$	3.0×10^{-2}	9.6×10^{-3}	4.4×10^{-3}
#it(topolog.)	6	7	9
#it(shape)	0	1	2

5 Conclusion

Studying the results obtained for the various test cases, we observe a rather mesh-independent behavior of the TOPSHAPE-algorithm and typically only a small number of iterations until successful termination. In all runs the topological derivative allows to find an approximation of the active set which is already very close to the optimal one. The subsequent shape optimization phase therefore only has to adjust locally. Concerning the positive weights α_1 and α_2 we note that the solution upon termination of the algorithm is of course independent of the choice of the weights. However, they might influence the speed of convergence. In our tests, we found that the method is rather robust with respect to the weights α_1 and α_2. It turned out to be useful to have $\alpha_1, \alpha_2 \in (0, 1)$ such that J_3 is slightly emphasized.

Appendix A: Topological sensitivity in the 2d case

In this section we prove the formula obtained for the topological derivative in Sect. 2.1. For an initial domain $\mathcal{I}$ and a small "hole" ω_ε, the perturbed domain is defined as $\mathcal{I}_\varepsilon = \mathcal{I} \setminus \omega_\varepsilon$. The strategy consists in defining a sequence of approximations of the perturbed solution. Each approximation fulfills the boundary conditions either on the outer boundary $\partial\mathcal{I}$ or on the inner boundary $\partial\omega_\varepsilon$, but never on both at the same time. Therefore, at the step n of the approximation procedure, the approximation leaves a small discrepancy either on the inner or the outer boundary which is compensated by the next approximation, and so on. In some cases we can define an approximation of u_ε of the form

$$u_\varepsilon(x) = \sum_{i=1}^{n} \varepsilon^i \left(v_i(x) + w_i\left(\frac{x}{\varepsilon}\right)\right) + r_{n+1}(x, \varepsilon)$$

with $r_{n+1}(x, \varepsilon) = O(\varepsilon^{n+1})$. In general, however, the form of the expansion of u_ε can be more complex. Usually, if $\mathcal{I}_\varepsilon$ is a domain with a small hole of size ε, the first approximation will be given by the solution on the domain without a hole. Then the error induced near the small hole ω_ε will be compensated by a boundary layer located in a neighborhood of the hole ω_ε. In the following calculations, we use the techniques and results as described in [19]. For the subsequent expansions to hold true we rely on local regularity results for elliptic partial differential equations; see, e.g., Theorem 9.7 in [1].

A.1 Case 1: "Active hole in inactive set"

A small hole is created in the inactive set $\mathcal{I}_1$ yielding mixed Dirichlet-Neumann boundary conditions. The small hole perturbs the solution u of (2.10)–(2.12) defined on $\mathcal{I}_1$, but it also has an effect on v, the solution of (2.16)–(2.17), through the boundary conditions (2.17). In what follows, we write $\mathcal{I}$ instead of $\mathcal{I}_1$.

Let $\mathcal{I}$ and ω, with $0 \in \omega$, $0 \in \mathcal{I}$, be two open bounded subsets of $\mathbb{R}^2$ with smooth boundaries. For $\varepsilon > 0$ we define the perturbed domains $\mathcal{I}_\varepsilon$ and ω_ε by $\omega_\varepsilon := \{x \in \mathbb{R}^2 : x = \varepsilon\xi,\ \xi \in \omega\}$ and $\mathcal{I}_\varepsilon := \mathcal{I} \setminus \omega_\varepsilon$. We consider the perturbed problem in $\mathbb{R}^2$ with $f \in L^2(\mathcal{I})$ and $\psi \in H^2(\mathcal{I})$:

$$-\Delta u_\varepsilon(x) = f(x) \quad \text{in } \mathcal{I}_\varepsilon, \tag{A.71}$$

$$u_\varepsilon(x) = 0 \quad \text{on } \Sigma, \tag{A.72}$$

$$\partial_n u_\varepsilon(x) = \partial_n \psi(x) \quad \text{on } \partial\mathcal{I}_\varepsilon \setminus \Sigma. \tag{A.73}$$

We want to expand the functional

$$J_1(\mathcal{I}_\varepsilon) = \int_{\mathcal{I}_\varepsilon} \max(0, u_\varepsilon(x) - \psi(x))^2 \, dx \tag{A.74}$$

with respect to ε. Here we adopt the notation introduced in Sect. 2.1. We also assume that ω is the open ball of radius 1 in $\mathbb{R}^2$. However, it is noted that the following calculations can be easily adapted for more general shapes. With this, we are interested in performing the asymptotic expansion of the solution of

$$-\Delta \tilde{u}_\varepsilon(x) = g(x) \quad \text{in } \mathcal{I}_\varepsilon, \tag{A.75}$$

$$\tilde{u}_\varepsilon(x) = -\psi(x) \quad \text{on } \Sigma, \tag{A.76}$$

$$\partial_n \tilde{u}_\varepsilon(x) = 0 \quad \text{on } \partial\mathcal{I}_\varepsilon \setminus \Sigma. \tag{A.77}$$

A.1.1 Expansion of u: first limit problem

The first approximation we consider is the solution of (A.75)–(A.77) with $\varepsilon = 0$, i.e., when there is no hole:

$$-\Delta \tilde{u}(x) = g(x) \quad \text{in } \mathcal{I}, \tag{A.78}$$

$$\tilde{u}(x) = -\psi(x) \quad \text{on } \Sigma, \tag{A.79}$$

$$\partial_n \tilde{u}(x) = 0 \quad \text{on } \partial\mathcal{I} \setminus \Sigma. \tag{A.80}$$

We call (A.78)–(A.80) the *first limit problem*. Observe that the approximation $\tilde{u}$ violates the Neumann boundary condition (A.77) on the boundary of the hole ω_ε. The defect left by $\tilde{u}$ on $\partial\omega_\varepsilon$ is given by $\partial_n \tilde{u}(x)$. For $x \in \partial\omega_\varepsilon$ we have the expansion

$$\partial_n \tilde{u}(x) = \nabla \tilde{u}(0) \cdot n + D^2 \tilde{u}(0) x \cdot n + O(\varepsilon^2), \tag{A.81}$$

where n is the outward unit normal vector to $\mathcal{I}_\varepsilon$, and $D^2\tilde{u}$ is the Hessian of $\tilde{u}$. In what follows, we will write $\partial_{n_x} = \nabla_x \cdot n$ and $\partial_{n_\xi} = \nabla_\xi \cdot n$, where ∇_x and ∇_ξ are

the gradients with respect to the variables x and ξ, respectively. These gradients are related by $\varepsilon\nabla_x = \nabla_\xi$.

The first term of the defect (A.81) is written as

$$\nabla\tilde{u}(0)\cdot n = \sum_{j=1}^{2} \partial_j \tilde{u}(0)\partial_{n_x} x_j. \tag{A.82}$$

Since $x = -\varepsilon n$ on $\partial\omega_\varepsilon$, we get $D^2\tilde{u}(0)x\cdot n = -\varepsilon D^2\tilde{u}(0)n\cdot n$ and, thus,

$$D^2\tilde{u}(0)x\cdot n = -\varepsilon\sum_{j=1}^{2}(\partial_n x_j)^2\partial^2_{j,j}\tilde{u}(0) - 2\varepsilon\partial_n x_1\partial_n x_2\partial^2_{1,2}\tilde{u}(0). \tag{A.83}$$

Now we proceed to the next step of our approximation.

A.1.2 Second limit problems

The defect due to (A.82) in the expansion of $\tilde{u}_\varepsilon$ is compensated by

$$-\varepsilon\sum_{j=1}^{2}\partial_j\tilde{u}(0)W_j(\xi),$$

where W_j is the solution of the following system on the inflated domain $\mathbb{R}^2\setminus\omega$:

$$-\Delta_\xi W_j(\xi) = 0 \quad \text{in } \mathbb{R}^2\setminus\omega, \tag{A.84}$$

$$\partial_{n_\xi} W_j(\xi) = \partial_{n_\xi}\xi_j \quad \text{on } \partial\omega. \tag{A.85}$$

It can be easily verified that a solution is

$$W_j(\xi) = -\xi_j|\xi|^{-2}. \tag{A.86}$$

On the other hand, the defect due to (A.83) is compensated by

$$\varepsilon^2\left[\sum_{j=1}^{2}\partial^2_{j,j}\tilde{u}(0)q_j(\xi) + 2\partial^2_{1,2}\tilde{u}(0)q_{12}(\xi)\right]$$

with the functions q_j defined as solutions of

$$-\Delta_\xi q_j(\xi) = 0 \quad \text{in } \mathbb{R}^2\setminus\omega, \tag{A.87}$$

$$\partial_{n_\xi} q_j(\xi) = (\partial_{n_\xi}\xi_j)^2 \quad \text{on } \partial\omega. \tag{A.88}$$

The function q_{12} is a solution of

$$-\Delta_\xi q_{12}(\xi) = 0 \quad \text{in } \mathbb{R}^2\setminus\omega, \tag{A.89}$$

$$\partial_{n_\xi} q_{12}(\xi) = \partial_{n_\xi}\xi_1\partial_{n_\xi}\xi_2 \quad \text{on } \partial\omega. \tag{A.90}$$

Expressing ξ in polar coordinates (r, θ), i.e., $\xi = \xi(r, \theta)$, solutions of (A.87)–(A.88) and (A.89)–(A.90) are for $j = 1, 2$

$$q_j(\xi) = \frac{1}{4r^2}\cos 2\theta - \frac{\ln r}{2} + \lambda_j, \tag{A.91}$$

$$q_{12}(\xi) = \frac{1}{4r^2}\sin 2\theta + \lambda_{12}. \tag{A.92}$$

The constant λ_j, $j = 1, 2$, is fixed to remove the singularity due to the logarithmic term; see (A.107) below. Further, $\lambda_{12} = 0$ turns out to be appropriate; see p. 560. Summarizing, our first approximation of the solution u_ε is

$$\tilde{u}_\varepsilon(x) \backsimeq \tilde{u}(x) - \varepsilon \sum_{j=1}^{2} \partial_j \tilde{u}(0) W_j(\xi) + \varepsilon^2 \left[\sum_{j=1}^{2} \partial^2_{j,j} \tilde{u}(0) q_j(\xi) + 2\partial^2_{1,2} \tilde{u}(0) q_{12}(\xi) \right]. \tag{A.93}$$

This approximation now leaves a defect of order ε^2 on the outer boundary $\partial\mathcal{I}$. Therefore, a new limit problem must be introduced to compensate for this defect.

A.1.3 Third limit problems

On the outer boundary $\partial\mathcal{I}$, the function $W_j(\xi)$ given by (A.86) is equal to

$$W_j(\xi = \varepsilon^{-1}x) = -\varepsilon\, x_j |x|^{-2}.$$

As a consequence, the defect due to the W_j-term in the first approximation (A.93) becomes

$$\varepsilon^2 \sum_{j=1}^{2} \partial_j \tilde{u}(0)\, x_j |x|^{-2} + o(\varepsilon^2),$$

which will be compensated with the help of functions $\mathcal{G}_j$ defined by

$$-\Delta \mathcal{G}_j(x) = 0 \quad \text{in } \mathcal{I}, \tag{A.94}$$

$$\mathcal{G}_j(x) = x_j |x|^{-2} \quad \text{on } \Sigma, \tag{A.95}$$

$$\partial_n \mathcal{G}_j(x) = \partial_n (x_j |x|^{-2}) \quad \text{on } \partial\mathcal{I} \setminus \Sigma. \tag{A.96}$$

The functions q_1 and q_2 leave a defect of order ε^2 on the Neumann boundary $\partial\mathcal{I} \setminus \Sigma$. To correct this defect, we need to introduce the following problem:

$$-\Delta S(x) = 0 \quad \text{in } \mathcal{I}, \tag{A.97}$$

$$S(x) = 0 \quad \text{on } \Sigma, \tag{A.98}$$

$$2\partial_n S(x) = \partial_n \ln |x| \quad \text{on } \partial\mathcal{I} \setminus \Sigma. \tag{A.99}$$

Consequently, the final approximation of the solution $\tilde{u}_\varepsilon$ is

$$\tilde{u}_\varepsilon(x) = \tilde{u}(x) + w_\varepsilon(x) + o(\varepsilon^2), \tag{A.100}$$

with w_ε defined by

$$\begin{aligned} w_\varepsilon(x) = -\varepsilon \sum_{j=1}^{2} \partial_j \tilde{u}(0) \big[W_j(\xi) + \varepsilon \mathcal{G}_j(x) \big] \\ + \varepsilon^2 \sum_{j=1}^{2} \partial_{j,j}^2 \tilde{u}(0)[q_j(\xi) + S(x)] + 2\partial_{1,2}^2 \tilde{u}(0) q_{12}(\xi). \end{aligned}$$

Now we are ready to calculate the expansion of the cost functional (A.74). First note that (A.100) implies

$$\begin{aligned} J_1(\mathcal{I}_\varepsilon) &= \int_{\mathcal{I}_\varepsilon} \max(0, \tilde{u}(x))^2 \, dx + \int_{\mathcal{I}_\varepsilon} 2 \max(0, \tilde{u}(x)) w_\varepsilon \, dx + o(\varepsilon^2) \\ &= J_1(\mathcal{I}) - \int_{\omega_\varepsilon} \max(0, \tilde{u}(x))^2 + \int_{\mathcal{I}_\varepsilon} 2 \max(0, \tilde{u}(x)) w_\varepsilon(x) + o(\varepsilon^2). \end{aligned} \tag{A.101}$$

Further observe that

$$\int_{\omega_\varepsilon} \max(0, \tilde{u}(x))^2 \, dx = \pi \varepsilon^2 \max(0, \tilde{u}(0))^2 + o(\varepsilon^2).$$

It remains to study the term $\int_{\mathcal{I}_\varepsilon} 2 \max(0, \tilde{u}(x)) w_\varepsilon \, dx$ in (A.101). As in (2.34)–(2.38) we introduce the adjoint states p_u and p_v. Applying Green's formula we get

$$\begin{aligned} \int_{\mathcal{I}_\varepsilon} -\Delta p_u(x) W_j(\xi) \, dx = -\int_{\partial\omega_\varepsilon} \partial_{n_x} p_u(x) W_j(\xi) - p_u(x) \partial_{n_x} W_j(\xi) \, dx \\ - \int_{\partial\mathcal{I}} \partial_{n_x} p_u(x) W_j(\xi) \, dx + \int_{\partial\mathcal{I}\setminus\Sigma} p_u(x) \partial_{n_x} W_j(\xi) \, dx. \end{aligned}$$

Using $x = \varepsilon\xi$ we obtain

$$\int_{\partial\omega_\varepsilon} \partial_{n_x} p_u(x) W_j(\xi) \, dx = -\int_{\partial\omega} \big(\partial_{n_x} p_u(0) + O(\varepsilon) \big) \frac{\xi_j}{|\xi|^2} \varepsilon \, d\xi. \tag{A.102}$$

Since $n = -(\cos\theta, \sin\theta)$ and $\xi |\xi|^{-2} = -n$ on $\partial\omega$, for $j = 1$ we get

$$\begin{aligned} \int_{\partial\omega_\varepsilon} \partial_{n_x} p_u(x) W_1(\xi) \, dx &= \varepsilon \int_{\partial\omega} \big[\partial_1 p_u(0) + O(\varepsilon) \big] \cos^2\theta \, d\xi \\ &= \pi \varepsilon \partial_1 p_u(0) + O(\varepsilon^2) \end{aligned}$$

and further

$$\begin{aligned}
&\int_{\partial\omega_\varepsilon} p_u(x)\partial_{n_x} W_1(\xi)\,dx \\
&\quad= \int_{\partial\omega} \varepsilon^{-1}\partial_{n_\xi} W_1(\xi)\Big[p_u(0)+\varepsilon\xi\cdot\nabla p_u(0)+O(\varepsilon^2)\Big]\varepsilon\,d\xi \\
&\quad= -p_u(0)\int_{\partial\omega}\cos\theta\,d\xi-\varepsilon\int_{\partial\omega}[\partial_1 p_u(0)\cos\theta+\partial_2 p_u(0)\sin\theta]\cos\theta\,d\xi+O(\varepsilon^2) \\
&\quad= -\pi\varepsilon\partial_1 p_u(0)+O(\varepsilon^2).
\end{aligned}$$

A similar result holds true for $j=2$. From these two cases we conclude

$$\begin{aligned}
\int_{\mathcal{I}_\varepsilon} -\Delta p_u(x) W_j(\xi)\,dx = -2\pi\varepsilon\partial_j p_u(0) - \int_{\partial\mathcal{I}} \partial_{n_x} p_u(x) W_j(\xi)\,dx \\
+\int_{\partial\mathcal{I}\setminus\Sigma} p_u(x)\partial_{n_x} W_j(\xi)\,dx + O(\varepsilon^2). \qquad \text{(A.103)}
\end{aligned}$$

Again by applying Green's formula, we continue by studying the term

$$\begin{aligned}
\int_{\mathcal{I}_\varepsilon} -\Delta p_u(x)\mathcal{G}_j(x)\,dx = -\int_{\partial\omega_\varepsilon} \partial_{n_x} p_u(x)\mathcal{G}_j(x) - p_u(x)\partial_{n_x}\mathcal{G}_j(x)\,dx \\
-\int_{\partial\mathcal{I}} \partial_{n_x} p_u(x)\mathcal{G}_j(x)\,dx + \int_{\partial\mathcal{I}\setminus\Sigma} p_u(x)\partial_{n_x}\mathcal{G}_j(x)\,dx. \qquad \text{(A.104)}
\end{aligned}$$

Equations (A.94)–(A.95) yield

$$-\int_\Sigma \partial_{n_x} p_u(x) W_j(\xi)\,dx - \varepsilon\int_\Sigma \partial_{n_x} p_u(x)\mathcal{G}_j(x)\,dx = 0,$$

and further

$$\int_{\partial\mathcal{I}\setminus\Sigma} p_u(x)\partial_{n_x} W_j(\xi)\,dx + \varepsilon\int_{\partial\mathcal{I}\setminus\Sigma} p_u(x)\partial_{n_x}\mathcal{G}_j(x)\,dx = 0.$$

Consequently, adding (A.103) and ε-times (A.104) we obtain

$$\begin{aligned}
&\int_{\mathcal{I}_\varepsilon} -\Delta p_u(x)(W_j(\xi)+\varepsilon\mathcal{G}_j(x))\,dx \\
&\quad= -2\pi\varepsilon\partial_j p_u(0) - \int_{\partial\mathcal{I}\setminus\Sigma} \partial_{n_x} p_u(x)\big[W_j(\xi)+\varepsilon\mathcal{G}_j(x)\big]\,dx + O(\varepsilon^2). \qquad \text{(A.105)}
\end{aligned}$$

Similarly, for the other terms we have by Green's formula

$$\begin{aligned}
\int_{\mathcal{I}_\varepsilon} -\Delta p_u(x) q_j(\xi)\,dx = -\int_{\partial\omega_\varepsilon} \partial_{n_x} p_u(x) q_j(\xi) - p_u(x)\partial_{n_x} q_j(\xi)\,dx \\
-\int_{\partial\mathcal{I}} \partial_{n_x} p_u(x) q_j(\xi)\,dx + \int_{\partial\mathcal{I}\setminus\Sigma} p_u(x)\partial_{n_x} q_j(\xi)\,dx.
\end{aligned}$$

We study the last three terms separately. Since $\partial_{n_x} p_u(x)$ and $q_j(\xi)$ are bounded on $\partial\omega_\varepsilon$ with respect to ε we infer

$$\int_{\partial\omega_\varepsilon} \partial_{n_x} p_u(x) q_j(\xi)\, dx = O(\varepsilon). \tag{A.106}$$

Then, for $j = 1$ and in view of $\partial_{n_\xi} \xi_1 = -\cos\theta$ we get

$$\begin{aligned}\int_{\partial\omega_\varepsilon} p_u(x)\partial_{n_x} q_1(\xi)\, dx &= \int_{\partial\omega} \varepsilon^{-1}\partial_{n_\xi} q_1(\xi)\big[p_u(0) + O(\varepsilon)\big]\varepsilon\, d\xi \\ &= p_u(0)\int_{\partial\omega} \cos^2\theta\, d\xi + O(\varepsilon) = \pi p_u(0) + O(\varepsilon);\end{aligned}$$

and similarly for $j = 2$. According to (A.91) and in view of $r = |\xi| = |x|\varepsilon^{-1}$ we have

$$\int_\Sigma \partial_{n_x} p_u(x) q_j(\xi)\, dx = \int_\Sigma \partial_{n_x} p_u(x)\left(\frac{\varepsilon^2}{4|x|^2}\cos 2\theta - \frac{\ln|x| - \ln\varepsilon}{2} + \lambda_j\right) dx.$$

Fixing for $j = 1, 2$

$$\lambda_j(\varepsilon) = \frac{\int_\Sigma \partial_{n_x} p_u(x)(\ln|x| - \ln\varepsilon)\, dx}{2\int_\Sigma \partial_{n_x} p_u(x)\, dx} \tag{A.107}$$

we obtain

$$\int_\Sigma \partial_{n_x} p_u(x) q_j(\xi)\, dx = O(\varepsilon).$$

If $\int_\Sigma \partial_{n_x} p_u(x)\, dx \neq 0$ then (A.107) is well-defined; otherwise one readily finds $\mathcal{T}_1 \equiv 0$. At this point we have

$$\begin{aligned}\int_{\mathcal{I}_\varepsilon} -\Delta p_u(x) q_j(\xi)\, dx &= \pi p_u(0) + O(\varepsilon) \\ &\quad - \int_{\partial\mathcal{I}\setminus\Sigma} \partial_{n_x} p_u(x) q_j(\xi)\, dx + \int_{\partial\mathcal{I}\setminus\Sigma} p_u(x)\partial_{n_x} q_j(\xi)\, dx.\end{aligned}$$

With the help of the function S (cf. (A.97)–(A.99)) we find

$$\begin{aligned}&\int_{\mathcal{I}_\varepsilon} -\Delta p_u(x)(q_j(\xi) + S(x))\, dx \\ &\quad = \pi p_u(0) + O(\varepsilon) - \int_{\partial\mathcal{I}\setminus\Sigma} \partial_{n_x} p_u(x)(q_j(\xi) + S(x))\, dx.\end{aligned} \tag{A.108}$$

Finally, by Green's formula

$$\begin{aligned}\int_{\mathcal{I}_\varepsilon} -\Delta p_u(x) q_{12}(\xi)\, dx &= -\int_{\partial\omega_\varepsilon} \partial_{n_x} p_u(x) q_{12}(\xi) - p_u(x)\partial_{n_x} q_{12}(\xi)\, dx \\ &\quad - \int_{\partial\mathcal{I}} \partial_{n_x} p_u(x) q_{12}(\xi)\, dx + \int_{\partial\mathcal{I}\setminus\Sigma} p_u(x)\partial_{n_x} q_{12}(\xi)\, dx.\end{aligned}$$

As before, due to boundedness on $\partial\omega_\varepsilon$ we have

$$\int_{\partial\omega_\varepsilon} \partial_{n_x} p_u(x) q_{12}(\xi)\, dx = O(\varepsilon). \tag{A.109}$$

Next, expanding $p_u(x)$ about 0 we find

$$\begin{aligned}\int_{\partial\omega_\varepsilon} p_u(x)\partial_{n_x} q_{12}(\xi)\, dx &= \int_{\partial\omega} \varepsilon^{-1}\partial_{n_\xi} q_{12}(\xi)\big[p_u(0) + O(\varepsilon)\big]\varepsilon\, d\xi \\ &= p_u(0)\int_{\partial\omega} \cos\theta \sin\theta\, d\xi + O(\varepsilon) = O(\varepsilon).\end{aligned}$$

Choosing $\lambda_{12} = 0$ in (A.92) and considering $r = \varepsilon^{-1}|x|$, we get

$$-\int_\Sigma \partial_{n_x} p_u(x) q_{12}(\xi)\, dx + \int_{\partial\mathcal{I}\setminus\Sigma} p_u(x)\partial_{n_x} q_{12}(\xi)\, dx = O(\varepsilon).$$

We finally obtain

$$\int_{\mathcal{I}_\varepsilon} -\Delta p_u(x) q_{12}(\xi)\, dx = -\int_{\partial\mathcal{I}\setminus\Sigma} \partial_{n_x} p_u(x) q_{12}(\xi)\, dx + O(\varepsilon). \tag{A.110}$$

Now (A.110), (A.108) and (A.105) yield

$$\begin{aligned}&\int_{\mathcal{I}_\varepsilon} 2\max(0,\tilde{u}(x)) w_\varepsilon(x)\, dx \\ &= -\int_{\mathcal{I}_\varepsilon} \Delta p_u(x) w_\varepsilon(x)\, dx \\ &= -\varepsilon\sum_{j=1}^{2} \partial_j\tilde{u}(0)[-2\pi\varepsilon\partial_j p_u(0) + O(\varepsilon^2)] + 2\varepsilon^2\partial^2_{1,2}\tilde{u}(0)[O(\varepsilon)] \\ &\quad + \varepsilon^2\sum_{j=1}^{2}\partial^2_{j,j}\tilde{u}(0)[\pi p_u(0) + O(\varepsilon)] - \int_{\partial\mathcal{I}\setminus\Sigma} \partial_{n_x} p_u(x) w_\varepsilon(x)\, dx \\ &= 2\pi\varepsilon^2\nabla\tilde{u}(0)\cdot\nabla p_u(0) + \pi\varepsilon^2 p_u(0)\left(\sum_{j=1}^{2}\partial^2_{j,j}\tilde{u}(0)\right) + o(\varepsilon^2) \\ &\quad - \int_{\partial\mathcal{I}\setminus\Sigma} \partial_{n_x} p_u(x) w_\varepsilon(x)\, dx.\end{aligned}$$

Since $\sum_{j=1}^2 \partial^2_{j,j}\tilde{u}(0) = -g(0)$, we obtain

$$\begin{aligned}\int_{\mathcal{I}_\varepsilon} 2\max(0,\tilde{u}(x)) w_\varepsilon(x)\, dx &= \pi\varepsilon^2[2\nabla\tilde{u}(0)\cdot\nabla p_u(0) - p_u(0)g(0)] \\ &\quad - \int_{\partial\mathcal{I}\setminus\Sigma} \partial_{n_x} p_u(x) w_\varepsilon(x)\, dx.\end{aligned} \tag{A.111}$$

A.1.4 Expansion of v

We also have to derive an asymptotic expansion of the solution of

$$-\Delta v_\varepsilon(x) = -\Delta\psi(x) \quad \text{in } \mathcal{A}_\varepsilon, \tag{A.112}$$

$$v_\varepsilon(x) = u_\varepsilon(x) \quad \text{on } \partial\mathcal{A}_\varepsilon \tag{A.113}$$

with $\mathcal{A}_\varepsilon := \mathcal{A} \cup \omega_\varepsilon$. Again we define $\tilde{v}_\varepsilon = v_\varepsilon - \psi$ and consider the system

$$-\Delta\tilde{v}_\varepsilon(x) = 0 \quad \text{in } \mathcal{A}_\varepsilon, \tag{A.114}$$

$$\tilde{v}_\varepsilon(x) = \tilde{u}_\varepsilon(x) \quad \text{on } \partial\mathcal{A}_\varepsilon. \tag{A.115}$$

Similar to the expansion (A.100) we get

$$\tilde{v}_\varepsilon(x) = \tilde{v}(x) + z_\varepsilon(x) + o(\varepsilon^2),$$

where z_ε is the solution of

$$-\Delta z_\varepsilon(x) = 0 \quad \text{in } \mathcal{A}_\varepsilon, \tag{A.116}$$

$$z_\varepsilon(x) = w_\varepsilon(x) \quad \text{on } \partial\mathcal{A}_\varepsilon. \tag{A.117}$$

The expansion of the functional

$$J_2(\mathcal{A}_\varepsilon) = \int_{\mathcal{A}\cup\omega_\varepsilon} \min(0, \tilde{v}_\varepsilon(x))^2\, dx \tag{A.118}$$

relies on the adjoint state p_v from (2.34)–(2.35). Similar to the computations for J_1 we obtain

$$\begin{aligned} J_2(\mathcal{A}_\varepsilon) &= \int_{\mathcal{A}_\varepsilon} \min(0, \tilde{v}(x))^2\, dx + \int_{\mathcal{A}} 2\min(0, \tilde{v}(x)) z_\varepsilon\, dx + o(\varepsilon^2) \\ &= J_2(\mathcal{A}) + \int_{\omega_\varepsilon} \min(0, \tilde{v}(x))^2\, dx - \int_{\mathcal{A}} \Delta p_v(x) z_\varepsilon\, dx + o(\varepsilon^2) \\ &= J_2(\mathcal{A}) + \pi\varepsilon^2 \min(0, \tilde{u}(0))^2 - \int_{\partial\mathcal{A}} \partial_{n_\mathcal{A}} p_v(x) z_\varepsilon\, dx + o(\varepsilon^2). \end{aligned}$$

A.1.5 Expansion of J_1 and J_2

Gathering the results of (A.111) and of Sect. A.1.4, we get the expansion

$$\begin{aligned} &J_1(\mathcal{I}_\varepsilon) + J_2(\mathcal{A}_\varepsilon) \\ &\quad = J_1(\mathcal{I}) + J_2(\mathcal{A}) \\ &\qquad + \pi\varepsilon^2[2\nabla\tilde{u}(0)\cdot\nabla p_u(0) - p_u(0)g(0) - \max(0, \tilde{u}(0))^2 + \min(0, \tilde{u}(0))^2] \\ &\qquad + o(\varepsilon^2) - \int_{\partial\mathcal{I}\setminus\Sigma} \partial_{n_x} p_u(x) w_\varepsilon(x)\, dx - \int_{\partial\mathcal{A}} \partial_{n_\mathcal{A}} p_v(x) z_\varepsilon\, dx. \end{aligned}$$

In view of (2.36)–(2.38), $\partial\mathcal{A}_\varepsilon = \partial\mathcal{A} \cup \partial\omega_\varepsilon$, $\partial\mathcal{I} \setminus \Sigma = \partial\mathcal{A}$ and (A.117) we have

$$\begin{aligned} &J_1(\mathcal{I}_\varepsilon) + J_2(\mathcal{A}_\varepsilon) \\ &\quad = J_1(\mathcal{I}) + J_2(\mathcal{A}) + \pi\varepsilon^2[2\nabla\tilde{u}(0)\cdot\nabla p_u(0) \\ &\qquad - p_u(0)g(0) - \max(0,\tilde{u}(0))^2 + \min(0,\tilde{u}(0))^2] + o(\varepsilon^2). \end{aligned} \tag{A.119}$$

Recalling our notational convention from (2.9), we summarize our result in the following theorem.

Theorem 3 *The cost functionals* (2.6) *and* (2.7) *admit the following expansion for a small perturbation of the inactive set* $\mathcal{I}_1$:

$$J_1(\mathcal{I}_\varepsilon) + J_2(\mathcal{A}_\varepsilon) = J_1(\mathcal{I}_1) + J_2(\mathcal{A}) + \pi\varepsilon^2\mathcal{T}_1(x_0) + \pi\varepsilon^2\mathcal{T}_2(x_0) + o(\varepsilon^2),$$

with the topological derivatives $\mathcal{T}_1$ *and* $\mathcal{T}_2$ *given by*

$$\begin{aligned} \mathcal{T}_1(x_0) &= 2\nabla(u-\psi)(x_0)\cdot\nabla p_u(x_0) - p_u(x_0)(f+\Delta\psi)(x_0) \\ &\quad - \max(0,(u-\psi)(x_0))^2, \\ \mathcal{T}_2(x_0) &= \min(0,u(x_0)-\psi(x_0))^2, \end{aligned}$$

where x_0 *is the center of* ω_ε *and the adjoint state* p_u *satisfies* (2.36)–(2.38).

A.2 Case 2: "Inactive hole in active set"

Since the approximation in this case is very similar to the one of Sect. A.1, we do not repeat the details. We only point to the fact that the Dirichlet conditions on the holes may suggest that a singular situation with respect to the leading term in $\ln\varepsilon$ occurs in the expansion of the functionals. However, the situation is different here because the Dirichlet value on the boundary of the small hole is asymptotically the value of the solution v of (2.16)–(2.17) at the center of the hole. As a consequence, the $\ln\varepsilon$-term disappears and we end up with an approximation similar to the one in Sect. A.1. In fact, we have the following result.

Theorem 4 *The cost functionals* (2.6) *and* (2.7) *admit the following expansion for a small perturbation of the active set* $\mathcal{A}$

$$J_1(\mathcal{I}_\varepsilon) + J_2(\mathcal{A}_\varepsilon) = J_1(\mathcal{I}) + J_2(\mathcal{A}) + \pi\varepsilon^2\mathcal{T}_1(x_0) + \pi\varepsilon^2\mathcal{T}_2(x_0) + o(\varepsilon^2),$$

with the topological derivatives $\mathcal{T}_1$ *and* $\mathcal{T}_2$ *given by*

$$\begin{aligned} \mathcal{T}_1(x_0) &= \max(0,v(x_0)-\psi(x_0))^2, \\ \mathcal{T}_2(x_0) &= 2\nabla(v-\psi)(x_0)\cdot\nabla p_v(x_0) - \min(0,(v-\psi)(x_0))^2, \end{aligned}$$

where x_0 *is the center of* ω_ε *and* p_v *satisfies* (2.34)–(2.35).

A.3 Case 3: "Active hole in inactive island"

In the case where the inactive set is split into several connected components we have to deal with one or several "islands" with Neumann boundary conditions. Several difficulties appear in this situation. First of all, we need to take into account the compatibility conditions for the initial equation but also for the approximation and the adjoint state. This leads to a more involved approximation procedure when compared to the other cases. Depending on the compatibility condition for the adjoint problem, we need to choose a normalisation for the initial Neumann problem. When creating a hole in $\mathcal{I}$ we would have to consider a problem similar to (A.71)–(A.73), but with Neumann conditions on the boundary $\partial\omega_\varepsilon$:

$$-\Delta u_\varepsilon(x) = f(x) \quad \text{in } \mathcal{I}_\varepsilon,$$
$$\partial_n u_\varepsilon(x) = \partial_n \psi(x) \quad \text{on } \partial\mathcal{I}_\varepsilon.$$

Its solvability hinges on the usual compatibility condition for Neumann problems; see, e.g., [6]. In order to always guarantee existence of a solution we rather consider the problem

$$-\Delta u_\varepsilon(x) = f(x) - \frac{1}{|\mathcal{I}_\varepsilon|}\int_{\mathcal{I}_\varepsilon} g(y)\,dy \quad \text{in } \mathcal{I}_\varepsilon, \tag{A.120}$$

$$\partial_n u_\varepsilon(x) = \partial_n \psi(x) \quad \text{on } \partial\mathcal{I}_\varepsilon, \tag{A.121}$$

with $g(x) = f(x) + \Delta\psi(x)$ instead. It can readily be checked that the right-hand side of (A.120)–(A.121) fulfills the usual compatibility condition. Then $\tilde{u}_\varepsilon = u_\varepsilon - \psi$ solves

$$-\Delta \tilde{u}_\varepsilon(x) = \bar{g}_\varepsilon(x) \quad \text{in } \mathcal{I}_\varepsilon, \tag{A.122}$$

$$\partial_n \tilde{u}_\varepsilon(x) = 0 \quad \text{on } \partial\mathcal{I}_\varepsilon, \tag{A.123}$$

where $\bar{g}_\varepsilon$ denotes the mean value

$$\bar{g}_\varepsilon(x) = g(x) - \frac{1}{|\mathcal{I}_\varepsilon|}\int_{\mathcal{I}_\varepsilon} g(y)\,dy.$$

Observe that this mean value admits the expansion

$$\bar{g}_\varepsilon(x) = \bar{g}(x) + \frac{\pi\varepsilon^2}{|\mathcal{I}|}\bar{g}(0) + o(\varepsilon^2). \tag{A.124}$$

As in the previous sections we proceed by studying limit problems. In this context, the first approximation which we consider is the solution of (A.122)–(A.123) with $\varepsilon = 0$, i.e., the case when there is no hole:

$$-\Delta \tilde{u}(x) = \bar{g}(x) \quad \text{in } \mathcal{I}, \tag{A.125}$$

$$\partial_n \tilde{u}(x) = 0 \quad \text{on } \partial\mathcal{I}. \tag{A.126}$$

We call (A.125)–(A.126) the first limit problem. Of course, the compatibility condi-

tion is fulfilled for (A.125)–(A.126). The difference $\tilde{u}_\varepsilon - \tilde{u}$ solves

$$-\Delta(\tilde{u}_\varepsilon - \tilde{u}) = \bar{g}_\varepsilon - \bar{g} \quad \text{in } \mathcal{I}, \tag{A.127}$$

$$\partial_n(\tilde{u}_\varepsilon - \tilde{u}) = -\partial_n\tilde{u} \quad \text{on } \partial\omega_\varepsilon, \tag{A.128}$$

$$\partial_n(\tilde{u}_\varepsilon - \tilde{u}) = 0 \quad \text{on } \partial\mathcal{I}. \tag{A.129}$$

In view of (A.81) we approximate (A.127)–(A.129) by the sum of the following two Neumann problems:

$$-\Delta z_1(x) = 0 \quad \text{in } \mathcal{I}, \tag{A.130}$$

$$\partial_n z_1(x) = -\partial_n\tilde{u}(0) \quad \text{on } \partial\omega_\varepsilon, \tag{A.131}$$

$$\partial_n z_1(x) = 0 \quad \text{on } \partial\mathcal{I}, \tag{A.132}$$

and

$$-\Delta z_2(x) = \frac{\pi\varepsilon^2}{|\mathcal{I}|}\bar{g}(0) \quad \text{in } \mathcal{I}, \tag{A.133}$$

$$\partial_n z_2(x) = -D^2\tilde{u}(0)x \cdot n \quad \text{on } \partial\omega_\varepsilon, \tag{A.134}$$

$$\partial_n z_2(x) = 0 \quad \text{on } \partial\mathcal{I}. \tag{A.135}$$

It can be checked that the compatibility conditions are fulfilled for both problems. We further have $\tilde{u}_\varepsilon - \tilde{u} = z_1 + z_2 + o(\varepsilon^2)$. As for the Dirichlet problem, z_1 is first approximated by $-\varepsilon\sum_{j=1}^2 \partial_j u(0) W_j(\xi)$, where W_j is the solution of (A.84)–(A.85). The discrepancy induced by W_j on $\partial\mathcal{I}$ is then compensated with the help of $\mathcal{G}_j$ satisfying

$$-\Delta\mathcal{G}_j(x) = 0 \quad \text{in } \mathcal{I}, \tag{A.136}$$

$$\partial_n\mathcal{G}_j(x) = \partial_n(x_j|x|^{-2}) \quad \text{on } \partial\mathcal{I}. \tag{A.137}$$

The right-hand side of (A.136)–(A.137) fulfills the compatibility conditions. Thus, an approximation of z_1 is given by

$$z_1(x) = -\varepsilon\sum_{j=1}^{2} \partial_j\tilde{u}(0)[W_j(\xi) + \varepsilon\mathcal{G}_j(x)] + o(\varepsilon^2). \tag{A.138}$$

Recall that the change of variables $x = \varepsilon\xi$ implies $\Delta_x = \varepsilon^{-2}\Delta_\xi$ and $\nabla_x = \varepsilon^{-1}\nabla_\xi$. Now, in order to solve (A.133)–(A.135), we introduce $v_\varepsilon(\xi)$ corresponding to $z_2(x)$ as the solution of

$$-\Delta_\xi v_\varepsilon(\xi) = \frac{\pi\varepsilon^4}{|\mathcal{I}|}\bar{g}(0) \quad \text{in } \mathbb{R}^2 \setminus \omega, \tag{A.139}$$

$$\begin{aligned}\partial_{n_\xi} v_\varepsilon(\xi) = {} & \varepsilon^2[\cos^2\theta\,\partial_{11}^2\tilde{u}(0) + \sin^2\theta\,\partial_{22}^2\tilde{u}(0)] \\ & + 2\varepsilon^2\sin\theta\cos\theta\,\partial_{12}^2\tilde{u}(0) \quad \text{on } \partial\omega.\end{aligned} \tag{A.140}$$

Since $2\cos^2\theta = 1+\cos 2\theta$, $2\sin^2\theta = 1-\cos 2\theta$, and $\partial^2_{11}\tilde{u}(0)+\partial^2_{22}\tilde{u}(0) = -\bar{g}(0)$, the solution of (A.139)–(A.140) is given by

$$v_\varepsilon(\xi) = \frac{\pi\varepsilon^4}{4|\mathcal{I}|}\bar{g}(0)r^2 + \left(\frac{\varepsilon^2}{2}\bar{g}(0) - \frac{\pi\varepsilon^4}{2|\mathcal{I}|}\bar{g}(0)\right)\ln r + \beta_\varepsilon$$
$$+ \frac{\varepsilon^2}{4r^2}\left(\partial^2_{11}\tilde{u}(0)\cos 2\theta - \partial^2_{22}\tilde{u}(0)\cos 2\theta + \partial^2_{12}\tilde{u}(0)\sin 2\theta\right).$$

The constant β_ε will be properly chosen below. The approximation $v_\varepsilon(\xi)$ leaves a discrepancy of order ε^2 on $\partial\mathcal{I}$. To correct this defect, we introduce the following problem:

$$-\Delta S_\varepsilon(x) = 0 \quad \text{in } \mathcal{I}, \tag{A.141}$$

$$\partial_n S_\varepsilon(x) = \frac{\pi\varepsilon^2}{4|\mathcal{I}|}\bar{g}(0)\partial_n|x|^2 - \frac{\varepsilon^2}{2}\bar{g}(0)\partial_n \ln|x| \quad \text{on } \partial\mathcal{I}. \tag{A.142}$$

The compatibility condition for (A.141)–(A.142) is satisfied. Indeed, thanks to Green's formula we have

$$\int_{\partial\mathcal{I}} \partial_n|x|^2\,dx = 4|\mathcal{I}|$$

and

$$\int_{\partial\mathcal{I}} \partial_n \ln|x|\,dx = -\int_{\partial\omega_\varepsilon} \partial_n \ln|x|\,dx = 2\pi,$$

such that

$$\int_{\partial\mathcal{I}} \frac{\varepsilon^2\pi}{4|\mathcal{I}|}\bar{g}(0)\partial_n|x|^2 - \frac{\varepsilon^2}{2}\bar{g}(0)\partial_n\ln|x|\,dx = \pi\varepsilon^2\bar{g}(0) - \pi\varepsilon^2\bar{g}(0) = 0.$$

The approximation of the solution $\tilde{u}_\varepsilon$ is

$$\tilde{u}_\varepsilon(x) = \tilde{u}(x) + w_\varepsilon(x) + o(\varepsilon^2), \tag{A.143}$$

with w_ε defined by

$$w_\varepsilon(x) = -\varepsilon\sum_{j=1}^{2}\partial_j u(0)[W_j(\xi) + \varepsilon\mathcal{G}_j(x)] + v_\varepsilon(\xi) + S_\varepsilon(x).$$

Now we are ready to calculate the expansion of the cost functional (A.74). Using the expansion (A.143) we obtain

$$J_1(\mathcal{I}_\varepsilon) = J_1(\mathcal{I}) - \int_{\omega_\varepsilon}\max(0,\tilde{u}(x))^2 + \int_{\mathcal{I}_\varepsilon} 2\max(0,\tilde{u}(x))w_\varepsilon(x) + o(\varepsilon^2).$$

The adjoint state p_u is introduced in (2.39)–(2.40), where the right-hand side must fulfill the following compatibility condition

$$\int_{\mathcal{I}} 2\max(0,\tilde{u}(x))\,dx - \int_{\partial\mathcal{I}} \partial_{n_{\mathcal{A}}} p_v(x)\,dx = 0, \tag{A.144}$$

which can also be written as

$$\int_{\mathcal{I}} 2\max(0,\tilde{u}(x))\,dx + \int_{\mathcal{A}} 2\min(0,\tilde{v}(x))\,dx = 0. \tag{A.145}$$

Note that (A.145) imposes a normalisation condition on u. Now, in a similar way as in case 1, we get

$$\begin{aligned}
&\int_{\mathcal{I}_\varepsilon} -\Delta p_u(x) W_j(\xi)\,dx \\
&\quad = -2\pi\varepsilon\partial_j p_u(0) + \int_{\partial\mathcal{I}} p_u(x)\partial_{n_x} W_j(\xi)\,dx - \int_{\partial\mathcal{I}} \partial_{n_x} p_u(x) W_j(\xi)\,dx + O(\varepsilon^2)
\end{aligned}$$

and further

$$\int_{\mathcal{I}_\varepsilon} -\Delta p_u(x)\mathcal{G}_j(x)\,dx = \int_{\partial\mathcal{I}} p_u(x)\partial_{n_x}\mathcal{G}_j(x)\,dx - \int_{\partial\mathcal{I}} \partial_{n_x} p_u(x)\mathcal{G}_j(x)\,dx + O(\varepsilon).$$

Finally we have

$$\begin{aligned}
&\int_{\mathcal{I}_\varepsilon} -\Delta p_u(x) v_\varepsilon(\xi)\,dx \\
&\quad = -\int_{\partial\omega_\varepsilon} \partial_{n_x} p_u(x) v_\varepsilon(\xi) - p_u(x)\partial_{n_x} v_\varepsilon(\xi)\,dx \\
&\qquad + \int_{\partial\mathcal{I}} p_u(x)\partial_{n_x} v_\varepsilon(\xi)\,dx + \frac{\pi\varepsilon^2}{|\mathcal{I}|}\bar{g}(0)\int_{\mathcal{I}_\varepsilon} p_u(x)\,dx - \int_{\partial\mathcal{I}} \partial_{n_x} p_u(x) v_\varepsilon(\xi)\,dx \\
&\quad = -\beta_\varepsilon \int_{\partial\omega_\varepsilon} \partial_{n_x} p_u(x)\,dx - \pi\varepsilon^2\bar{g}(0)p_u(0) + \int_{\partial\mathcal{I}} p_u(x)\partial_{n_x} v_\varepsilon(\xi)\,dx \\
&\qquad + \frac{\pi\varepsilon^2}{|\mathcal{I}|}\bar{g}(0)\int_{\mathcal{I}_\varepsilon} p_u(x)\,dx - \int_{\partial\mathcal{I}} \partial_{n_x} p_u(x) v_\varepsilon(\xi)\,dx + o(\varepsilon^2).
\end{aligned}$$

We choose $\beta_\varepsilon = 0$ and find

$$\begin{aligned}
&\int_{\mathcal{I}_\varepsilon} -\Delta p_u(x) v_\varepsilon(\xi)\,dx \\
&\quad = -\pi\varepsilon^2\bar{g}(0)\bar{p}_u(0) + \int_{\partial\mathcal{I}} p_u(x)\partial_{n_x} v_\varepsilon(\xi)\,dx - \int_{\partial\mathcal{I}} \partial_{n_x} p_u(x) v_\varepsilon(\xi)\,dx + o(\varepsilon^2),
\end{aligned} \tag{A.146}$$

where $\bar{p}_u(0) = p_u(0) - |\mathcal{I}|^{-1} \int_{\mathcal{I}} p_u(x)dx$. We also have

$$\int_{\mathcal{I}_\varepsilon} -\Delta p_u(x) S_\varepsilon(x)\, dx = \int_{\partial\mathcal{I}} p_u(x)\partial_{n_x} v_\varepsilon(\xi)\, dx - \int_{\partial\mathcal{I}} \partial_{n_x} p_u(x) S_\varepsilon(x)\, dx + o(\varepsilon^2). \quad \text{(A.147)}$$

Collecting (A.146)–(A.147), we obtain

$$\int_{\mathcal{I}_\varepsilon} \Delta p_u(x) w_\varepsilon(x) = \pi\varepsilon^2[2\nabla\tilde{u}(0)\cdot\nabla p_u(0) - \bar{p}_u(0)\bar{g}(0)] - \int_{\partial\mathcal{I}} \partial_{n_x} p_u(x) w_\varepsilon(\xi)\, dx + o(\varepsilon^2). \quad \text{(A.148)}$$

A.3.1 Expansion of J_1 and J_2

In a similar way as in Sect. A.1.5, we get the following result from (A.148) and Sect. A.1.4.

Theorem 5 *The cost functionals (2.6) and (2.7) admit the following expansion for a small perturbation of the inactive set $\mathcal{I}_1$*

$$J_1(\mathcal{I}_\varepsilon) + J_2(\mathcal{A}_\varepsilon) = J_1(\mathcal{I}) + J_2(\mathcal{A}) + \pi\varepsilon^2\mathcal{T}_1(x_0) + \pi\varepsilon^2\mathcal{T}_2(x_0) + o(\varepsilon^2),$$

with the topological derivatives $\mathcal{T}_1$ and $\mathcal{T}_2$ given by

$$\mathcal{T}_1(x_0) = 2\nabla(u-\psi)(x_0)\cdot\nabla p_u(x_0) - \bar{p}_u(x_0)\bar{g}(x_0) - \max(0,(u-\psi)(x_0))^2,$$
$$\mathcal{T}_2(x_0) = \min(0, u(x_0) - \psi(x_0))^2,$$

where x_0 is the center of ω_ε and $\bar{p}_u$ and $\bar{g}$ are the mean values of p_u (cf. (2.39)–(2.40)) and g, respectively.

A.4 Expansion of J_3

The computation of J_3 is straightforward. If we are in case 1, no new island is created and the current islands are unchanged. Therefore the topological derivative $\mathcal{T}_3(x_0)$ is zero for all $x_0 \in \mathcal{I}_1$. In case 2, we create a new island ω_ε and, thus, we get the expansion

$$J_3(\mathcal{I}_\varepsilon) = J_3(\mathcal{I}) + \frac{1}{|\omega_\varepsilon|}\left(\int_{\omega_\varepsilon} g\right)^2 = \pi\varepsilon^2 g(x_0)^2 + o(\varepsilon^2).$$

We deduce the following expression for the topological derivative $\mathcal{T}_3(x)$ in case 2

$$\mathcal{T}_3(x_0) = g(x_0)^2 \quad \forall x \in \mathcal{A}.$$

In case 3, we modify an existing island. We can assume for simplicity that there is only one island $\mathcal{I}_2$. Then we get the expansion

$$\begin{aligned} J_3(\mathcal{I}_\varepsilon) &= \frac{1}{|\mathcal{I}_2 \setminus \omega_\varepsilon|} \left(\int_{\mathcal{I}_2 \setminus \omega_\varepsilon} g \right)^2 \\ &= \left(\frac{1}{|\mathcal{I}_2|} + \frac{\pi \varepsilon^2}{|\mathcal{I}_2|^2} + o(\varepsilon^2) \right) \left(\int_{\mathcal{I}_2} g - \pi \varepsilon^2 g(x_0) + o(\varepsilon^2) \right)^2 \\ &= J_3(\mathcal{I}) + \frac{\pi \varepsilon^2}{|\mathcal{I}_i|} \left(\int_{\mathcal{I}_i} g \right) \cdot \left(\frac{1}{|\mathcal{I}_i|} \int_{\mathcal{I}_i} g - 2g(x_0) \right) + o(\varepsilon^2). \end{aligned}$$

From this we deduce the following expression for the topological derivative $\mathcal{T}_3(x_0)$ in case 3:

$$\mathcal{T}_3(x_0) = \frac{1}{|\mathcal{I}_i|} \left(\int_{\mathcal{I}_i} g \right) \cdot \left(\frac{1}{|\mathcal{I}_i|} \int_{\mathcal{I}_i} g - 2g(x_0) \right).$$

References

1. Agmon, S.: Lectures on Elliptic Boundary Value Problems. Van Nostrand Mathematical Study, vol. 2. Van Nostrand, Toronto (1965)
2. Dambrine, M., Vial, G.: On the influence of a boundary perforation on the Dirichlet energy. Control Cybern. **34**(1), 117–136 (2005)
3. Delfour, M., Zolesio, J.-P.: Shapes and Geometries. Analysis, Differential Calculus and Optimization. SIAM Advances in Design and Control. SIAM, Philadelphia (2001)
4. Eschenauer, H., Schumacher, A.: Bubble method for topology and shape optimization of structures. Struct. Optim. **8**, 42–51 (1994)
5. Garreau, S., Guillaume, P., Masmoudi, M.: The topological asymptotic for pde systems: the elasticity case. SIAM J. Control Optim. **39**, 1756–1778 (2001)
6. Hackbusch, W.: Elliptic Differential Equations. Springer Series in Computational Mathematics, vol. 18. Springer, Berlin (1992)
7. Hackbusch, W., Mittelmann, H.: On multigrid methods for variational inequalities. Numer. Math. **42**, 65–76 (1983)
8. Hintermüller, M., Kunisch, K.: Path-following methods for a class of constrained minimization problems in function space. SIAM J. Optim. **17**(1), 159–187 (2006)
9. Hintermüller, M., Kunisch, K.: Feasible and non-interior path-following in constrained minimization with low multiplier regularity. SIAM J. Control Optim. **45**(4), 1198–1221 (2006)
10. Hintermüller, M., Ring, W.: A level set approach for the solution of a state-constrained optimal control problem. Numer. Math. **98**, 135–166 (2004)
11. Hintermüller, M., Ito, K., Kunisch, K.: The primal-dual active set strategy as a semismooth Newton method. SIAM J. Optim. **13**, 865–888 (2003)
12. Hoppe, R.H.W.: Multigrid methods for variational inequalities. SIAM J. Numer. Anal. **24**, 1046–1065 (1987)
13. Hoppe, R.H.W.: Two-sided approximations for unilateral variational inequalities by multigrid methods. Optimization **18**, 867–881 (1987)
14. Hoppe, R.H.W., Kornhuber, R.: Adaptive multilevel methods for obstacle problems. SIAM J. Numer. Anal. **31**, 301–323 (1994)
15. Kinderlehrer, D., Stampacchia, G.: An Introduction to Variational Inequalities and Their Applications. Academic, New York (1980)
16. Kornhuber, R.: Monotone multigrid methods for elliptic variational inequalities I. Numer. Math. **69**, 167–184 (1994)
17. Kornhuber, R.: Monotone multigrid methods for elliptic variational inequalities II. Numer. Math. **72**, 481–499 (1996)

18. Kornhuber, R.: Adaptive Monotone Multigrid Methods for Nonlinear Variational Problems. Teubner, Stuttgart (1997)
19. Maz'ya, V., Nazarov, S.A., Plamenevskij, B.: Asymptotic Theory of Elliptic Boundary Value Problems in Singularly Perturbed Domains, vols. 1, 2. Birkhäuser, Basel (2000)
20. Osher, S., Fedkiw, R.: Level Set Methods and Dynamic Implicit Surfaces. Springer, New York (2004)
21. Osher, S., Sethian, J.: Fronts propagating with curvature-dependant speed: algorithms based on Hamilton-Jacobi formulation. J. Comput. Phys. **79**, 12–49 (1988)
22. Peng, D., Merriman, B., Osher, S., Zhao, H., Kang, M.: A pde-based fast local level set method. J. Comput. Phys. **155**, 410–438 (1999)
23. Sethian, J.A.: Level Set Methods and Fast Marching Methods, 2nd edn. Cambridge University Press, Cambridge (1999)
24. Smith, G.D.: Numerical Solution of Partial Differential Equations: Finite Difference Methods. Clarendon, Oxford (1993)
25. Sokolowski, J., Zochowski, A.: On the topological derivative in shape optimization. SIAM J. Control Optim. **37**(4), 1251–1272 (1999)
26. Sokolowski, J., Zolesio, J.-P.: Introduction to Shape Optimization. Springer Series in Computational Mathematics, vol. 16. Springer, Berlin (1992)
27. Tai, X.-C.: Convergence rate analysis of domain decomposition methods for obstacle problems. East-West J. Numer. Math. **9**, 233–252 (2001)
28. Tai, X.-C.: Rate of convergence for some constraint decomposition methods for nonlinear variational inequalities. Numer. Math. **93**, 755–786 (2003)
29. Tai, X.-C., Tseng, P.: Convergence rate analysis of an asynchronous space decomposition method for convex minimization. Math. Comput. **71**, 1105–1135 (2001)
30. Wloka, J.: Partielle Differentialgleichungen. Teubner, Stuttgart (1982)
31. Zhao, H.K., Chan, T., Merriman, B., Osher, S.: A variational level set approach to multi-phase motion. J. Comput. Phys. **122**, 179–195 (1996)